FINAL REPORT

Contract NASw 1997

6 Channel Photometric Observations From the CV 990 Aircraft

Lockheed

PALO ALTO RESEARCH LABORATORY

LOCKHEED MISSILES & SPACE COMPANY • A GROUP DIVISION OF LOCKHEED AIRCRAFT CORPORATION

PALO ALTO, CALIFORNIA

FINAL REPORT

Contract NASw 1997

6 Channel Photometric Observations
From the CV 990 Aircraft

Attachment: Preprint of paper entitled
"The Spatial Extent of
Aurorae in O(5577) and N_2^+
(4278) Emissions"

S. B. Mende
R. H. Eather

Lockheed Palo Alto Research Laboratory
3251 Hanover Street
Palo Alto, California 94304

26 June 1970

FINAL REPORT

Contract NASw 1997

6 Channel Photometric Observations
From the CV 990 Aircraft

Lockheed Palo Alto Research Laboratory
3251 Hanover Street
Palo Alto, California 94304

26 June 1970

Preparation of the experiment

Contractual agreements were completed in late August 1969 and problems relating to the installation of the observing instruments in the aircraft were pursued immediately.

A mounting structure was designed and constructed to produce adequate mechanical interface between the Lockheed photometers with the associated electronics and the NASA Convair 990 aircraft.

A review of the up-to-date auroral literature showed that the objectives of the experiments could be greatly enhanced if more channels were added to the Lockheed photometer. With the concurrence of the NASA Airborne Science Office, steps were taken to accommodate a 6 channel photometer experiment instead of the proposed 4 channel experiment. The additional two channel tilting filter photometer required for this extension was supplied by Lockheed.

During the middle part of November Lockheed personnel, Drs. R. H. Eather and S. B. Mende, spent some time at NASA Ames Research Center where the Lockheed Photometer System was installed in the aircraft.

The system in the flight qualified system had the following advanced features.

a. 6 channels of narrow band tilting filter type photometers. Tilting action could be independently controlled on each channel as desired.

b. Pulse counting rate meter, giving excellent noise rejection and particularly useful in aircraft RF environment.

c. Real time chart recorder recording and monitoring in addition to magnetic recording compatibility.

d. Signal averaging capability by digital memory for 4 channels. Filter scans could be integrated for hours in order to enhance signal-to-noise ratio.

e. Active refrigeration for minimizing phototube noise.

f. Simple in-flight absolute calibration capability with standard light source.

The system was installed to look vertically up through two 65° windows of the Convair 990. All installations were completed and the system was functioning perfectly prior to flight 1 on November 19, 1969.

Observations

For the first few flights both Lockheed investigators accompanied the experiment to ensure smooth trouble-free operation of the complete system. Soon it was found that the system operated better than anticipated and complete operation could be maintained by a single operator. From flight 9 onward only Dr. Eather flew to accompany the Lockheed experiment.

The high sensitivity of the instrument and the continuous recording capability and the absence of malfunctions enabled us to take data continuously for the entire time the viewing windows were open during the flights.

Data processing

All the data for the auroral flights were processed. The data from every channel were scaled at two minute intervals for all the flights except the first flight which was essentially a check out flight and never approached the auroral zone. The two minutes scalings were converted into punched computer cards.

The navigator's log book was obtained from the NASA Airborne Science Office and the position readings versus time were also converted into punched card format. A computer program was generated which interpolated the position of the airplane from the entries in the navigator's log and calculated geographic latitudes and longitudes at two minute intervals. This same program converted the photometer readings into absolute quantities allowing for conversion factors and calibration values. A sample print output is shown as Appendix 1 to this report. An explanation of the values in the tables is also enclosed.

Besides the universal time, geographic position and photometer values, the magnetic local time, the invariant latitude and L values were all calculated. To discriminate against other visible radiation sources the program was used to check for contaminations from the Milky Way and from solar radiation by calculating the local shadow height at the time of the observation.

This computer program was also enlarged to do a statistical analysis of the photometer data.

A complete printout output was submitted to the NASA Airborne Science Office in March 1970.

Data analysis

The flight path of the NASA Convair 990 is plotted on the invariant latitude and magnetic time frame of reference (Fig. 1). Fairly good coverage of the nightside was accomplished by the expedition and there were two Midday Auroral Flights. Since the auroral phenomenon is governed by parameters which are best referenced by the invariant latitude and magnetic time system, the calculation of these coordinates allowed the derivation of some average properties of the observed aurorae.

a. Confirmation of the "soft auroral zone" north of the nightside aurora, as discussed on the 1968 expedition. Referring to Fig. 2 the ratio of the 6300 emission to 4278 is plotted as a function of the invariant latitude. The high ratios of the high side are due to the soft electrons. There is a similar increase in the same ratio on the low equatorward side of the auroral zone. If this were real it would be a very significant discovery, but it is too early to say yet whether the statistics associated with this low latitude peak is good enough to be significant.

b. Discovery of an analogous soft zone near midday located at much higher latitudes than at night. The ratio of 6300/4278 is extremely high on the nightside of Fig. 2 indicating the precipitation of very low energy electrons.

c. Confirmation of the soft zone by plots of 5200/4278 ratios. See Fig. 3. The 5200 atomic nitrogen emission has a very long lifetime usually theoretically 26 hours. Our results show that the 5200Å emission follows auroral fluctuations with relatively short time scale. In order to satisfy realistic excitation rates the lifetime must be shorter than predicted from theory, notwithstanding quenching effects.

d. The position of the hydrogen auroral region with respect to the electron region, Fig. 4. The premidnight region was found to be the nearest to the equator. The post-midnight region shows a wider profile but no net northward motion is observed. The midday proton auroral zone is poleward of the night zone.

e. The 5995 O_2^+ emission accompanies high energy electron produced lower red border auroras. The systematic statistical analysis of this emission did not produce any discernible tendencies.

f. On a large number of flights the 5876A atomic He line was monitored. An emission near 5876 was often detected, but there was no doppler shift between zenith and horizon directions, and we concluded it was (8-2) OH, in agreement with earlier investigations.

g. Studies of the distribution of the proton emission with respect to the electron auroras. In every case where possible a direct plot of the H_β and 4278 was obtained as the plane was traveling in the north, south direction as a function of local time. The results of this investigation were presented at the A.G.U. meeting in Washington by Dr. Eather. Essentially the findings were that the proton aurora in the morning side is mixed up with the electron aurora and the proton crossover did not appear to be present contrary to suggestions in the literature by various authors.

h. The investigation of the spatial intensity distribution of aurora in N_2^+ 4278Å and OI 5577Å. A preprint of this investigation is enclosed. This paper is in the process of being submitted to the J.G.R.

Publications

Besides the publication at the A.G.U. meeting in Washington, D.C., just referred to, Drs. R. H. Eather and S. B. Mende gave the following two papers:

1. The Spatial Extent of Aurorae in N_2^+ 4278 and OI 5577 emissions.
2. The Preliminary Results of the Lockheed 6 Channel Photometer on the NASA Convair 990 Expedition.

At the close of the contract it is expected that more than one publication will be submitted covering the results discussed previously under points a-g in the data analysis sections.

Figure Captions

Fig. 1: Flight paths on the 1969 Convair Expedition, plotted on an invariant geomagnetic latitude-magnetic time grid.

Fig. 2: The ratio 6300 OI/4278 N_2^+, corrected for proton excitation and airglow, as a function of invariant latitude, for daytime and nighttime intervals.

Fig. 3: The ratio 5200 NI/4278 N_2^+ corrected for proton excitation and airglow, as a function of invariant latitude, for daytime and nighttime intervals.

Fig. 4: Averaged Hβ emission, as a function of invariant latitude, for three magnetic-time intervals.

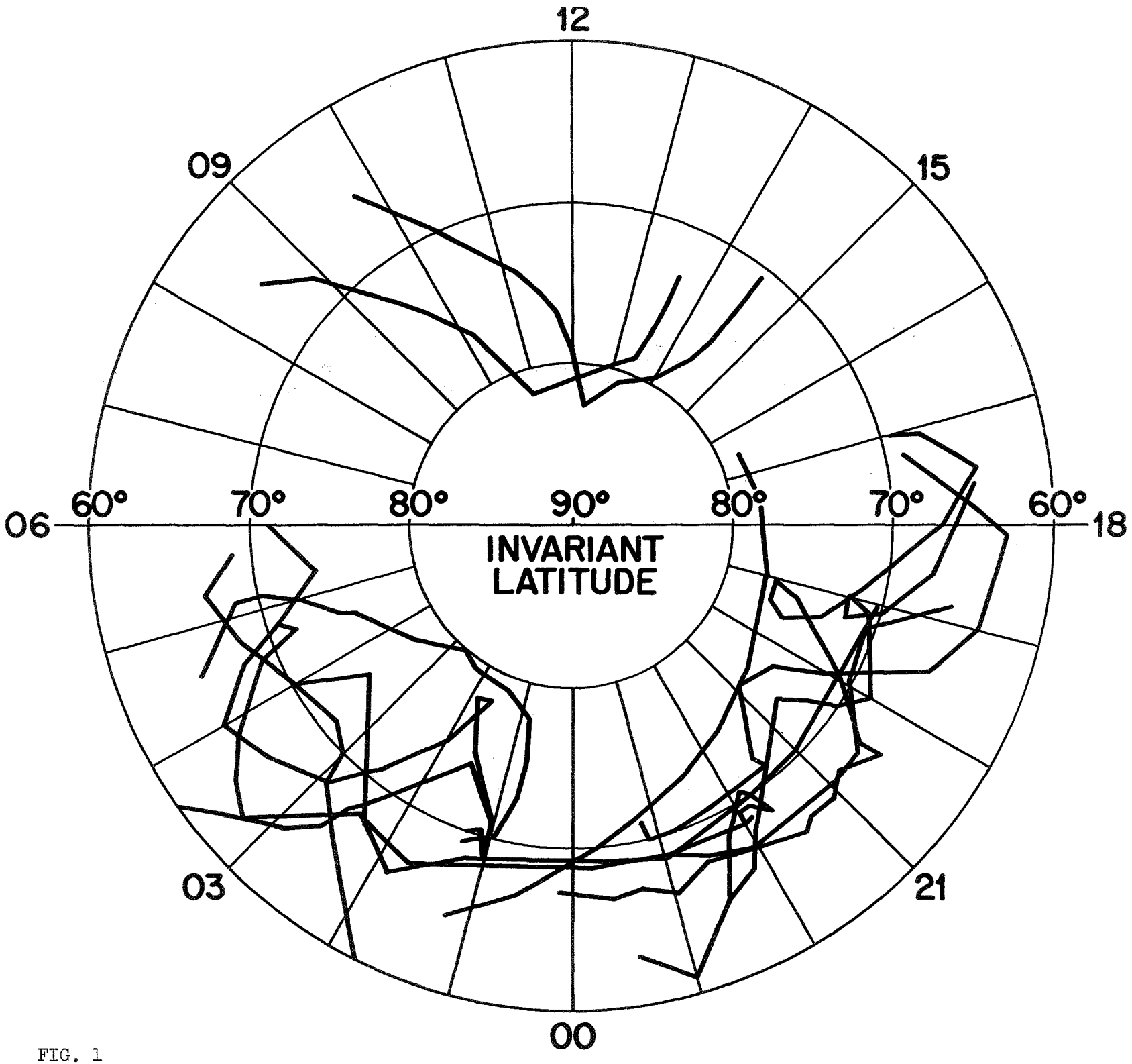
12
09
15
06
60°
70°
80°
90°
80°
70°
60°
18
INVARIANT
LATITUDE
03
21
00
MAGNETIC TIME

FIG. 1

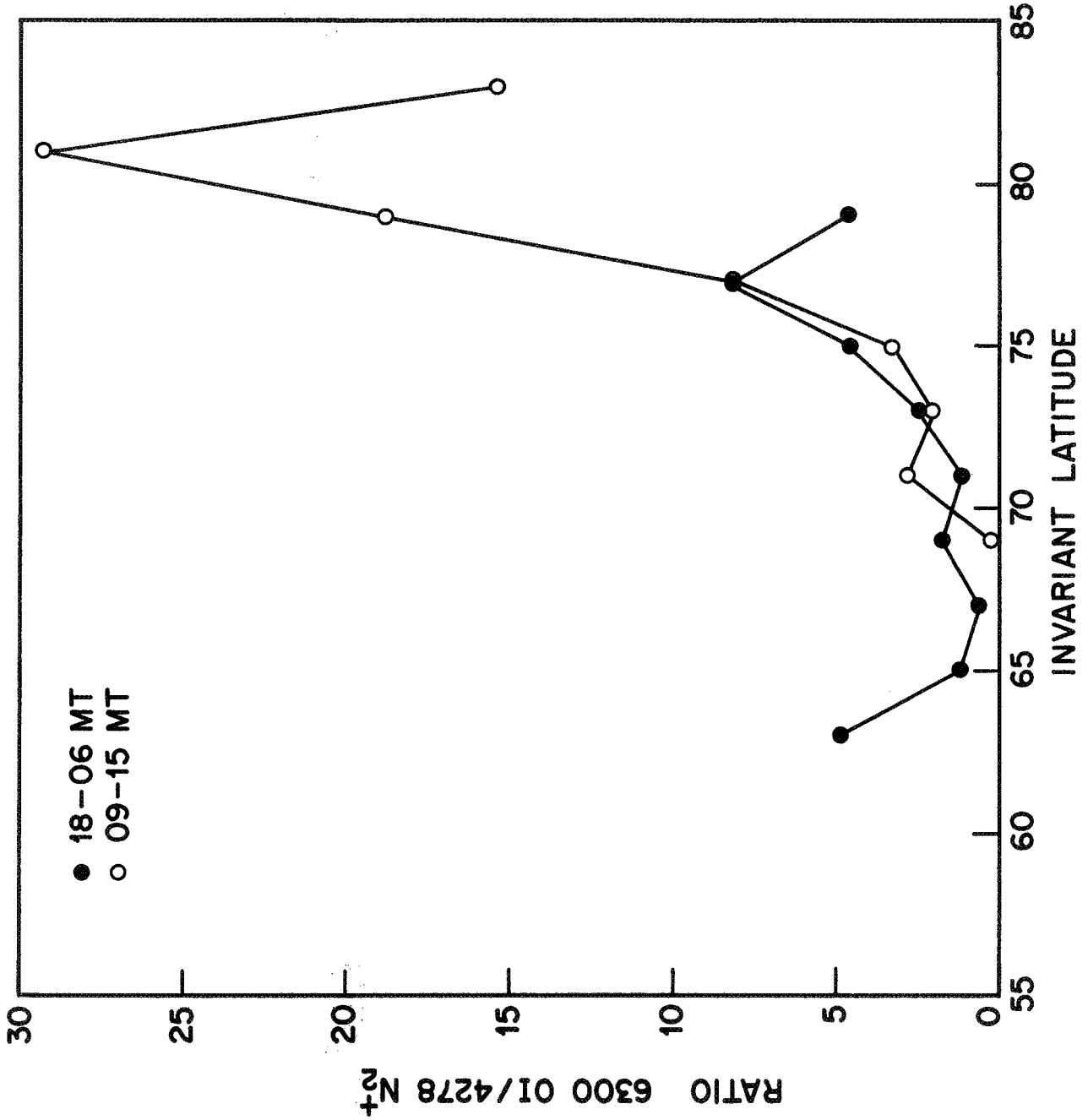
RATIO 6300 OI/4278 N_2^+
INVARIANT LATITUDE
18-06 MT
09-15 MT
0
5
10
15
20
25
30
55
60
65
70
75
80
85

FIG. 2

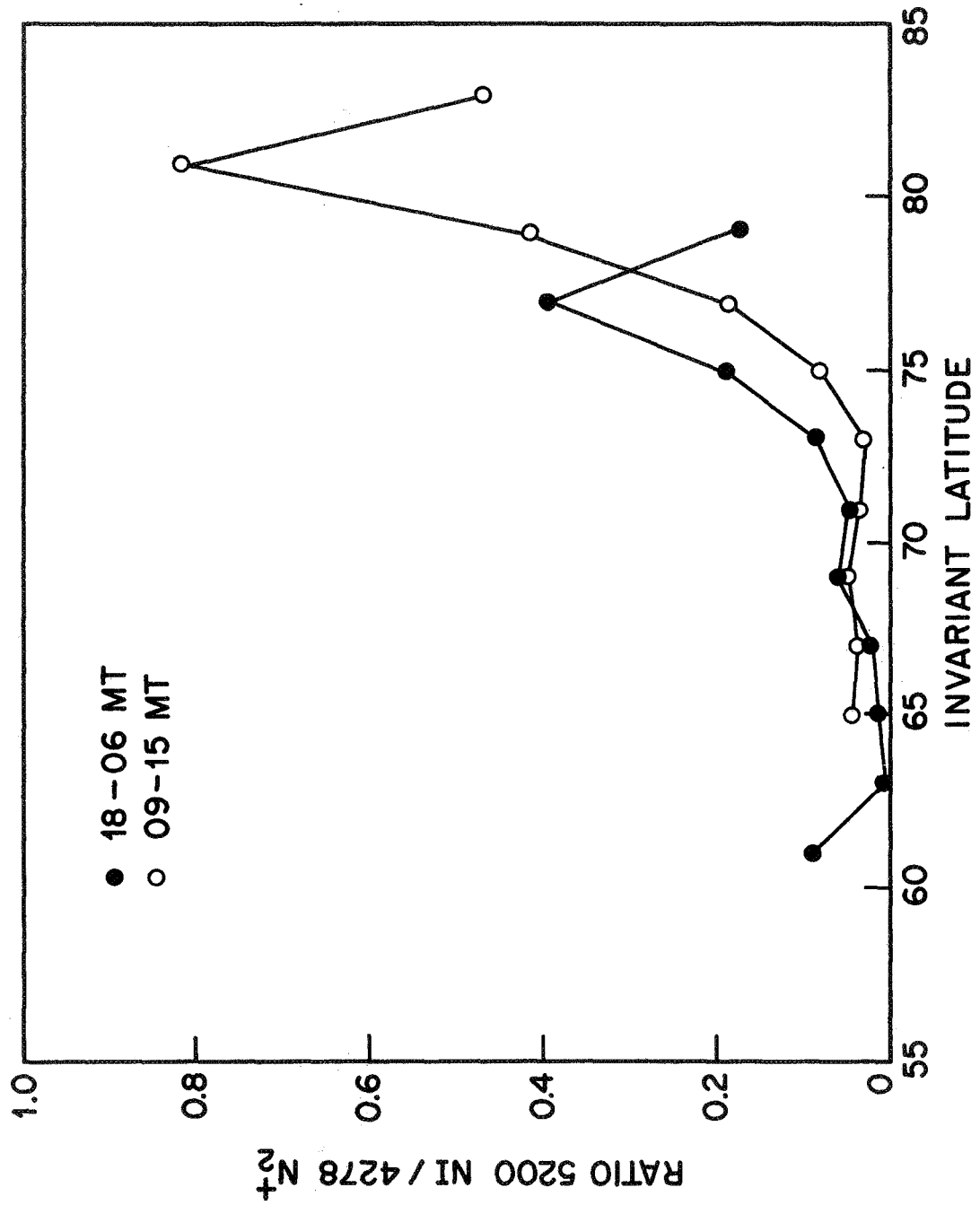
1.0
0.8
0.6
0.4
0.2
0
55
60
65
70
75
80
85
INVARIANT LATITUDE
RATIO 5200 NI / 4278 N_2^+
● 18-06 MT
○ 09-15 MT

FIG. 3

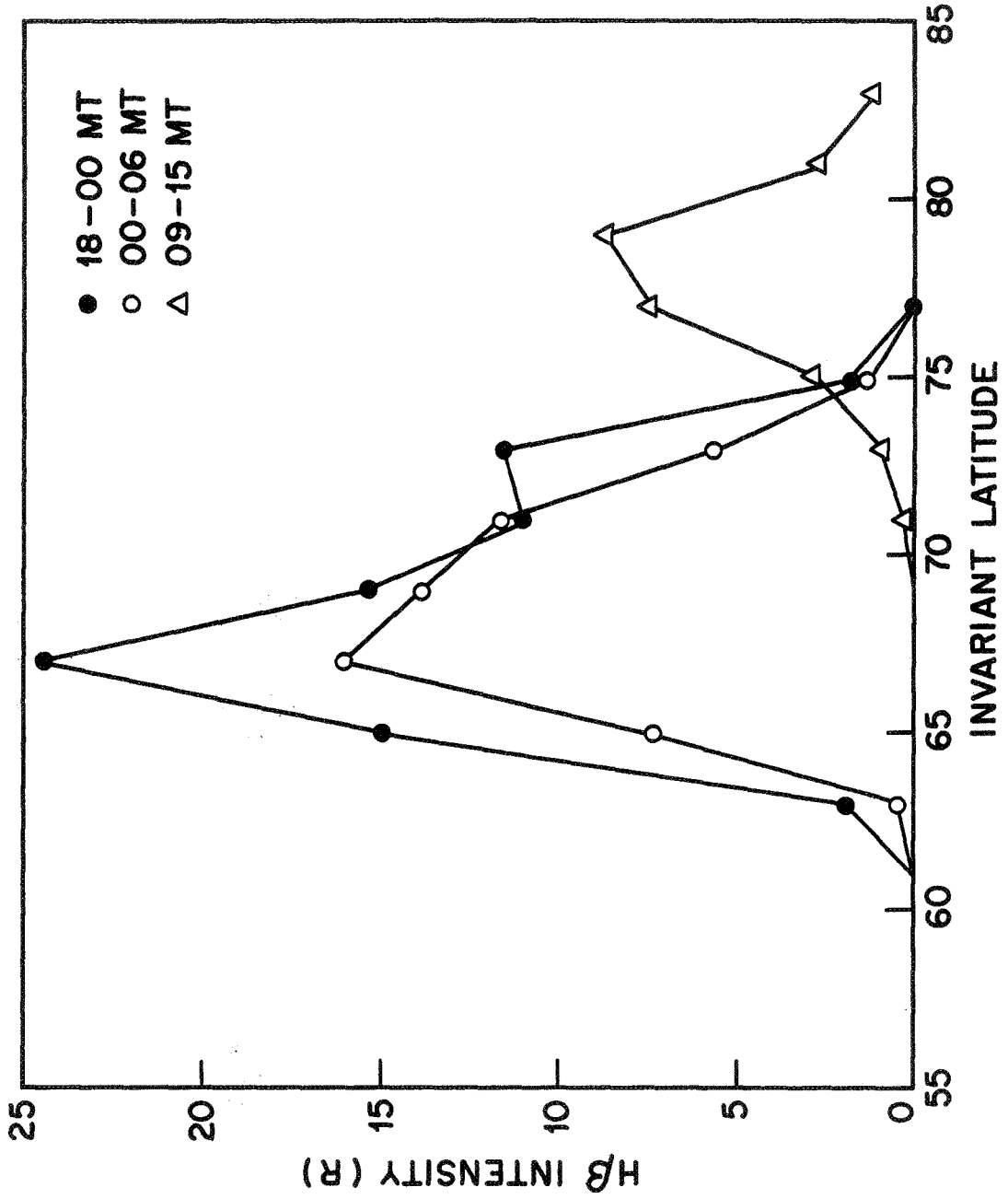
18–00 MT
00–06 MT
09–15 MT
Hβ INTENSITY (R)
INVARIANT LATITUDE
0
5
10
15
20
25
55
60
65
70
75
80
85

FIG. 4

APPENDIX 1

1969 NASA CONVAIR 990 AURORAL EXPEDITION

NAVIGATION DATA, ZENITH PHOTOMETERS (3 DEG. FULL ANGLE) AND STATISTICAL ANALYSIS

DESCRIPTION

NAVIGATION DATA WAS TAKEN FROM THE NAVIGATORS LOG, INTERPOLATIONS ARE MADE TO GIVE GEOGRAPHIC LATITUDE AND LONGITUDE AT 2 MINUTE INTERVALS THROUGHOUT THE FLIGHT, THE DATE AND UNIVERSAL TIME ARE USED TO COMPUTE THE SUBSOLAR LATITUDE AND LONGITUDE, THESE TWO QUANTITIES, ALONG WITH THE GEOGRAPHIC CO-ORDINATES, ARE USED TO CALCULATE THE MAGNETIC TIME.

MAGNETIC TIME IS DEFINED AS THE ANGLE BETWEEN THE MAGNETIC MERIDIAN WHICH PASSES THROUGH THE OBSERVATION POINT AND THE SUN (CHAMBERLAIN,1963 FRITZ AND GURNETT, 1965), AND IS GIVEN IN UNITS OF HOURS AND FRACTIONS OF AN HOUR.

THE GEOGRAPHIC CO-ORDINATES ARE THEN USED TO CALCULATE THE MCILWAIN 'L' PARAMETER (MCILWAIN,1963) AT AN ALTITUDE OF 100 KM, AND HENCE THE INVARIANT LATITUDE AS DEFINED BY

INVARIANT LATITUDE = INVERSECOSINE(1/SQRT(L))

A TEST IS MADE TO DETERMINE WHETHER THE MILKY WAS (AS OUTLINED IN NORTONS STAR ATLAS) WAS IN THE ZENITHAL FIELD OF VIEW. AN 'X' IS PRINTED IN THE COLUMN HEADED MW IF THIS WAS THE CASE.

PHOTOMETRIC READINGS FOR 6 ZENITHAL PHOTOMETERS WERE SCALED EVERY 2 MINS, IF THERE WERE RAPID TIME VARIATIONS IN A 2 MIN. PERIOD, AN AVERAGE INTENSITY WAS ESTIMATED. SMALL CORRECTIONS WERE APPLIED FOR WINDOW TRANSMISSION (8 PERCENT) AND ATMOSPHERIC EXTINCTION (APPROX. 5 PERCENT AT 33000 FT., DEPENDING ON WAVELENGTH).

THE LIGHT SOURCE CALIBRATION USED WAS A MEAN FROM A RADIOACTIVE LIGHT SOURCE SUPPLIED BY GADSDEN, AND A TUNGSTEN LAMP SUPPLIED BY FASTIE, THE READINGS FROM THE TWO SOURCES DID NOT DEVIATE FROM THE MEAN BY MORE THAN 10 PERCENT AT ANY WAVELENGTH.

ALL INTENSITIES ARE GIVEN IN RAYLEIGHS, AND ARE EMISSION INTENSITIES FOR THE PARTICULAR AURORAL OR AIRGLOW FEATURE, BACKGROUND CONTINUUM OR CONTAMINATION HAS BEEN SUBTRACTED USING THE TILTING FILTER METHOD, AN ESTIMATE OF THE 6300 AIRGLOW WAS SUBTRACTED BEFORE CALCULATING THE RATIO OF 6300 TO 4278, BECAUSE OF TEMPORAL AND SPATIAL VARIATIONS IN AIRGLOW ON A GIVEN NIGHT, THIS CORRECTION WILL OBVIOUSLY BE UNRELIABLE AT LOW INTENSITIES.

THE MILKY WAY WAS OFTEN IN THE ZENITH DURING THE PRE-MIDNIGHT HOURS (THIS WAS NOT A PROBLEM LAST EXPEDITION). MILKY WAY HBETA EMISSION CAN BE OF THE SAME ORDER AS AURORAL HBETA, SO IF A 'X' APPEARS IN THE MILKY WAY COLUMN, CHECK THE RELATIVE INTENSITY COLUMN, THESE INDICATE THE DEGREE OF POSSIBLE CONTAMINATION (FROM JOHNSONS MW HALPHA PLOTS), A '0' INDICATES NEGLIGIBLE CONTAMINATION, '1' MEANS SLIGHT, '2' MEANS POSSIBLY MODERATE AND '3' MEANS POSSIBLY STRONG, THERE IS A PROBABLE ERROR OF ABOUT 1 DEG. IN THE MW HALPHA LOCATIONS READ INTO THIS PROGRAM, SO ALLOW FOR 'EDGE EFFECTS'. IF MW CONTAMINATION IS A POSSIBLE PROBLEM CHECK THE RATIO OF HBETA TO 4278. IF THIS EXCEEDS ABOUT 0.4, IT IS A GOOD INDICATION OF AT LEAST SOME MILKY WAY CONTAMINATION.

SOME MEASUREMENTS WERE IN TWILIGHT PERIODS, THE SHADOW HEIGHT (CALCULATED WITH CORRECTIONS FOR THE NON-SPHERICAL EARTH) IS GIVEN IN THE FINAL COLUMN.

BECAUSE OF SENSITIVITY PROBLEMS WITH THE 5995 RECORDER CHANNEL, INTENSITIES BELOW 3R ARE NOT RELIABLE (3R CORRESPONDED TO 1MM CHART DEFLECTION). RANDOM ERRORS IN CHART SCALING (APPROX 1 MM) LEAD TO RANDOM ERRORS IN INTENSITY OF NOT MORE THAN 5 PERCENT, OR 1 R, WHICHEVER IS GREATER.

THE INDICATOR '' IN ANY COLUMN INDICATES THAT MEASUREMENTS WERE NOT TAKEN AT THAT WAVELENGTH AT THAT TIME, THE INDICATOR 9999 IN THE RATIO COLUMNS INDICATES THAT THE DENOMINATOR (4278) WAS ZERO, THE INDICATOR 8888 INDICATES THAT BOTH THE NUMERATOR AND DENOMINATOR WERE ZERO.

R.H. EATHER
LOCKHEED RESEARCH LABS
JANUARY, 1970

FLIGHT NUMBER 5 - NOVEMBER 29
ATS GRID

UT	GEOG. LAT.	GEOG. LONG.	MAG. TIME	INVAR. LAT.	L	WAVELENGTH 4278	4861	5200	5577	5995	6300	RATIO TO 4278 4861	5995	6300	MW	REL INT	SHADOW HEIGHT
208	58.75	94.07	18.82	70.11	8.64			WINDOW CLOSED									1292.6
210	58.75	93.64	18.89	70.17	8.69			WINDOW CLOSED									1334.1
212	58.75	93.22	18.97	70.21	8.73			WINDOW CLOSED									1376.4
214	58.75	92.80	19.04	70.26	8.77			WINDOW CLOSED									1419.5
216	58.75	92.37	19.12	70.31	8.81	30.0	.0	"	431.4	.0	234.1	.000	.00	5.14	X	2	1463.3
218	58.75	91.95	19.19	70.35	8.85	27.3	.0	"	400.6	.0	219.4	.000	.00	5.12	X	2	1507.9
220	58.75	91.52	19.27	70.40	8.88	23.2	.0	"	308.1	.0	204.8	.000	.00	5.39	X	0	1553.3
222	58.75	91.10	19.34	70.44	8.92	19.1	.0	"	277.3	.0	204.8	.000	.00	6.54	X	0	1599.3
224	58.75	90.68	19.42	70.48	8.96	15.0	.0	"	261.9	.0	219.4	.000	.00	9.30	X	0	1646.2
226	58.75	90.25	19.50	70.52	8.99	10.9	.0	"	246.5	.0	248.7	.000	.00	15.47	X	0	1693.7
228	58.75	89.83	19.57	70.55	9.02	10.9	.0	"	261.9	.0	248.7	.000	.00	15.47	X	0	1741.9
230	58.75	89.41	19.65	70.59	9.06	13.6	.0	"	277.3	.0	307.2	.000	.00	16.67	X	0	1790.9
232	58.73	88.98	19.73	70.61	9.07	15.0	.0	"	277.3	.0	256.0	.000	.00	11.74	X	0	1844.4
234	58.69	88.40	19.82	70.61	9.08	16.4	.0	"	277.3	.0	234.1	.000	.00	9.42	X	0	1902.9
236	58.65	87.96	19.91	70.61	9.09	19.1	.0	"	277.3	.0	190.2	.000	.00	5.77	X	0	1962.5
238	58.61	87.53	20.00	70.61	9.07	16.4	.0	"	228.0	.0	204.8	.000	.00	7.63	X	0	2023.1
240	58.57	86.80	20.09	70.61	9.07	16.4	.0	"	228.0	.0	204.8	.000	.00	7.63	X	0	2084.7
242	58.53	86.27	20.18	70.60	9.07	10.9	.0	"	197.2	.0	160.9	.000	.00	7.42	X	0	2147.3
244	58.37	86.05	20.24	70.47	8.95	16.4	.0	"	252.7	.0	219.4	.000	.00	8.53	X	0	2200.7
246	58.10	86.14	20.27	70.21	8.73	49.1	.0	"	554.6	.0	438.9	.000	.00	7.31	X	0	2244.8
248	57.83	86.23	20.31	69.95	8.51	20.8	2.1	"	306.4	3.7	214.1	.103	.18	6.43	X	0	2289.9
250	57.57	86.32	20.34	69.70	8.31	56.3	2.1	"	722.4	9.2	228.7	.038	.16	2.64	X	0	2336.0
252	57.30	86.41	20.38	69.44	8.11	900.3	4.3	"	6436.5	110.8	1452.2	.005	.12	1.52	X	0	2383.2
254	57.03	86.50	20.42	69.18	7.92	198.4	4.3	"	1198.3	36.9	1086.5	.022	.19	5.07	X	0	2431.5
256	56.76	86.59	20.45	68.92	7.73	42.5	8.6	"	332.1	3.7	439.4	.202	.09	8.46	X	0	2480.8
258	56.50	86.70	20.48	68.68	7.56	302.2	12.8	"	2670.4	36.9	991.9	.042	.12	3.02	X	0	2528.6
300	56.25	86.81	20.52	68.43	7.40	84.9	17.1	"	479.3	.0	322.9	.202	.00	2.86	X	0	2577.5
302	55.99	86.92	20.55	68.18	7.24	17.2	19.3	"	338.9	.0	207.9	1.121	.00	7.44	X	0	2627.4
304	55.93	87.37	20.55	68.10	7.19	10.8	21.4	"	321.8	.0	202.5	1.990	.00	11.39	X	0	2636.1
306	55.87	87.82	20.54	68.01	7.13	11.1	23.5	"	323.2	.0	160.6	2.111	.00	7.23	X	0	2644.9
308	55.82	88.27	20.54	67.92	7.08	32.0	25.7	"	534.1	.0	374.7	.803	.00	9.21	X	0	2653.6
310	55.76	88.72	20.53	67.83	7.02	25.2	25.7	"	472.4	.0	374.7	1.020	.00	11.71	X	0	2662.4
312	55.70	89.17	20.53	67.74	6.97	38.8	25.7	"	657.3	.0	447.8	.662	.00	9.48	X	0	2671.3
314	55.64	89.62	20.53	67.64	6.91	.0	36.4	"	540.9	.0	384.5	9.999	88.88	99.99	X	0	2680.1
316	55.59	90.06	20.53	67.55	6.85	27.5	23.5	"	427.9	.0	380.0	.856	.00	10.91	X	0	2689.7
318	55.53	90.49	20.53	67.45	6.80	31.2	21.4	"	414.2	.0	348.9	.696	.00	8.62	X	0	2699.8
320	55.48	90.92	20.52	67.36	6.75	17.6	21.4	"	352.6	.0	239.1	1.218	.00	9.05	X	0	2710.1
322	55.42	91.35	20.52	67.25	6.69	24.0	19.3	"	400.5	.0	244.4	.803	.00	6.85	X	0	2720.4
324	55.37	91.78	20.52	67.15	6.64	23.6	17.1	"	417.7	.0	249.9	.726	.00	7.20	X	0	2730.7
326	55.32	92.21	20.52	67.05	6.59	19.5	17.1	"	371.4	.0	264.4	.878	.00	9.45	X	0	2741.0
328	55.26	92.64	20.52	66.96	6.53	23.2	15.0	"	373.2	.0	160.0	.646	.00	3.45	X	0	2751.4
330	55.21	93.07	20.52	66.86	6.48	29.6	12.8	"	359.5	.0	114.2	.433	.00	1.15	X	0	2761.9
332	55.15	93.50	20.52	66.76	6.42	29.2	10.7	"	315.0	.0	90.3	.366	.00	.35	X	0	2772.4
334	55.10	93.93	20.52	66.65	6.37	22.0	8.6	"	301.3	.0	92.0	.389	.00	.54	X	0	2782.9
336	55.04	94.36	20.52	66.54	6.31	14.8	6.4	"	287.6	.0	93.7	.433	.00	.92	X	0	2793.5
338	54.99	94.79	20.52	66.43	6.26	42.1	6.4	"	719.0	.0	280.2	.153	.00	4.76	X	0	2804.2

UT	GEOG. LAT.	GEOG. LONG.	MAG. TIME	INVAR. LAT.	L	WAVELENGTH 4278	4861	5200	5577	5995	6300	RATIO TO 4278 4861	5995	6300	MW	REL INT	SHADOW HEIGHT
340	54.93	95.22	20.53	66.32	6.20	6.0	6.4	**	195.1	.0	86.4	.803	.00	.79	X	0	2814.8
342	55.00	95.40	20.54	66.36	6.22	12.5	8.6	**	239.6	.0	124.9	.686	.00	3.60	X	0	2833.6
344	55.17	95.34	20.58	66.53	6.31	56.9	12.8	**	513.5	.0	180.0	.226	.00	1.76	X	0	2859.9
346	55.35	95.28	21.62	66.71	6.40	44.0	17.1	**	479.3	.0	140.1	.389	.00	1.36	X	0	2885.4
348	55.53	95.22	20.65	66.90	6.50	17.6	21.4	**	368.0	.0	92.8	1.218	.00	.73	X	0	2910.2
350	55.69	95.16	20.69	67.06	6.58	2.0	25.7	**	318.4	.0	89.4	12.819	.00	4.69			2935.8
352	55.84	95.09	21.73	67.21	6.67	.0	27.8	**	301.3	.0	95.0	9.999	88.88	99.99			2962.5
354	55.99	95.03	20.77	67.36	6.75	.0	27.8	**	316.7	.0	84.0	9.999	88.88	99.99			2988.4
356	56.14	94.96	20.80	67.51	6.84	.0	30.0	**	314.9	.0	71.4	9.999	88.88	99.99			3013.6
358	56.29	94.90	20.84	67.67	6.93	5.5	30.0	**	376.6	.0	73.7	5.430	.00	.00			3038.0
400	56.13	95.17	20.86	67.48	6.82	.0	32.1	**	313.2	.0	80.7	9.999	88.88	99.99			3073.5
402	56.67	95.77	20.86	66.96	6.53	.0	34.2	**	326.9	.0	60.7	9.999	88.88	99.99			3120.5
404	56.48	95.85	20.89	66.77	6.43	18.4	25.7	**	380.3	.0	67.5	1.399	.00	.00			3176.6
406	56.30	95.92	20.93	66.58	6.33	3.5	19.3	**	277.3	.0	76.2	5.430	.00	.00			3233.8
408	56.11	95.99	20.97	66.39	6.23	.0	12.8	**	174.6	.0	92.2	9.999	88.88	99.99			3292.1
410	54.92	96.06	21.01	66.13	6.14	.0	8.6	**	131.8	.0	99.3	9.999	88.88	99.99	X	0	3351.5
412	56.20	96.15	21.03	66.46	6.27	3.5	4.3	**	144.5	.0	109.3	1.218	.00	8.33			3347.7
414	56.48	96.23	21.06	66.71	6.40	4.5	2.1	**	136.9	.0	113.9	.477	.00	7.56			3342.6
416	56.76	96.32	21.10	66.97	6.53	11.3	2.1	**	167.8	.0	115.3	.189	.00	3.13			3336.5
418	56.67	96.28	21.10	67.07	6.58	7.6	4.3	**	181.4	.0	128.3	.563	.00	6.35			3363.9
420	56.97	96.23	21.14	67.18	6.65	8.8	10.7	**	222.5	.0	119.5	1.218	.00	4.50			3390.7
422	56.67	96.19	21.18	67.28	6.71	15.4	17.1	**	309.8	.0	110.8	1.110	.00	2.00			3416.7
424	56.17	96.15	21.21	67.39	6.76	4.7	25.7	**	333.8	.0	67.5	5.430	.00	.00			3442.0
426	56.27	96.10	21.25	67.49	6.82	.0	34.2	**	280.7	.0	46.1	9.999	88.88	99.99			3466.6
428	56.38	96.06	21.29	67.59	6.88	.0	34.2	**	280.7	.0	53.4	9.999	88.88	99.99			3490.4
430	56.48	96.02	21.33	67.70	6.94	.0	36.4	**	263.6	.0	70.0	9.999	88.88	99.99			3513.3
432	56.44	96.26	21.34	67.62	6.90	.0	34.2	**	619.6	.0	68.0	9.999	88.88	99.99			3538.3
434	56.39	96.51	21.36	67.55	6.86	.0	32.1	**	359.4	.0	66.6	9.999	88.88	99.99			3563.3
436	56.35	96.75	21.38	67.47	6.81	.0	32.1	**	297.8	.0	66.9	9.999	88.88	99.99			3588.5
438	56.01	96.92	21.41	67.12	6.61	.0	30.0	**	284.1	.0	56.8	9.999	88.88	99.99			3669.8
440	55.67	97.56	21.40	66.69	6.39	3.2	17.1	**	248.2	.0	77.9	5.430	.00	.00			3715.6
442	55.34	96.69	21.35	66.19	6.14	4.3	8.6	**	147.2	.0	84.7	1.990	.00	1.08			3722.6
444	55.18	98.72	21.37	65.99	6.04	6.6	6.4	**	155.1	.0	86.4	.968	.00	.96			3761.8
446	55.20	98.56	21.45	66.09	6.09	9.0	4.3	**	166.8	.0	90.0	.477	.00	.90			3834.2
448	55.23	98.09	21.52	66.19	6.13	.8	4.3	**	135.2	.0	77.1	5.430	.00	.00			3905.5
450	55.33	97.91	21.58	66.33	6.20	17.1	4.3	**	181.4	.0	91.7	.250	.00	.68			3945.5
452	55.52	97.74	21.62	66.52	6.30	16.6	8.6	**	239.6	.0	95.6	.517	.00	.94			3954.0
454	55.70	97.66	21.65	66.71	6.40	9.6	15.0	**	234.5	.0	79.6	1.565	.00	.00			3960.8
456	55.69	97.58	21.69	66.90	6.50	11.1	23.5	**	320.1	.0	61.8	2.111	.00	.00			3966.0
458	56.10	97.48	21.73	67.16	6.64	5.5	30.0	**	469.0	.0	49.4	5.430	.00	.00			3966.6
500	56.31	97.39	21.77	67.33	6.73	.0	30.0	**	345.8	.0	60.4	9.999	88.88	99.99			3965.5
502	56.51	97.29	21.80	67.55	6.86	.0	32.1	**	297.8	.0	66.0	9.999	88.88	99.99			3962.5
504	56.49	97.29	21.84	67.53	6.85	.0	32.1	**	220.8	.0	66.0	9.999	88.88	99.99			3997.5
506	56.48	97.29	21.88	67.51	6.84	.0	34.2	**	388.5	.0	60.7	9.999	88.88	99.99			4032.2
508	56.46	97.29	21.92	67.49	6.82	.0	36.4	**	226.6	.0	70.0	9.999	88.88	99.99			4066.5
510	56.16	97.44	21.95	67.18	6.65	.0	38.5	**	277.3	.0	86.6	9.999	88.88	99.99			4151.8
512	55.85	97.58	21.99	66.87	6.48	.0	32.1	**	344.0	.0	73.3	9.999	88.88	99.99			4239.0
514	55.78	97.64	22.02	66.78	6.44	3.9	21.4	**	275.6	.0	74.5	5.430	.00	.00			4283.8
516	55.48	97.77	22.06	66.42	6.25	.0	12.8	**	190.0	.0	77.6	9.999	88.88	99.99			4388.1
518	55.23	97.75	22.11	66.24	6.16	19.3	8.6	**	239.6	.0	110.3	.444	.00	1.57			4465.3
520	55.20	97.56	22.16	66.24	6.16	.0	12.8	**	97.6	.0	63.0	9.999	88.88	99.99			4512.5

UT	GEOG. LAT.	GEOG. LONG.	MAG. TIME	INVAR. LAT.	L	WAVELENGTH 4278	4861	5200	5577	5995	6300	RATIO TO 4278 4861	5995	6300	REL INT	SHADOW HEIGHT
522	55.18	97.41	22.21	66.24	6.16	4.1	15.0	"	249.9	.0	68.6	3.635	.00	.00		4558.7
524	55.26	97.28	22.26	66.34	6.21	7.5	25.7	"	395.4	.0	78.4	3.445	.00	.00		4575.4
526	55.45	97.18	22.30	66.54	6.31	.0	34.2	"	404.0	.0	97.3	9.999	88.88	99.99		4562.1
528	55.64	97.09	22.33	66.74	6.41	.0	34.2	"	388.5	.0	177.7	9.999	88.88	99.99		4546.8
530	55.83	96.99	22.37	66.94	6.52	.0	36.4	"	263.6	.0	172.4	9.999	88.88	99.99		4529.6
532	56.04	96.89	22.41	67.15	6.63	28.7	30.0	"	561.4	.0	217.7	1.044	.00	4.80		4505.7
534	56.25	96.80	22.45	67.37	6.75	59.2	25.7	"	718.9	.0	301.5	.433	.00	3.74		4480.0
536	56.46	96.71	22.48	67.58	6.88	25.2	25.7	"	518.7	.0	228.4	1.020	.00	5.89		4452.6
538	56.51	96.52	22.54	67.66	6.92	58.8	23.5	"	751.5	.0	284.9	.400	.00	3.48		4465.1
540	56.42	96.25	22.62	67.61	6.89	5.7	23.5	"	412.5	.0	204.5	4.132	.00	21.84		4517.8
542	56.21	96.17	22.65	67.42	6.78	4.3	23.5	"	397.1	.0	204.5	5.430	.00	28.71		4589.9
546	55.90	96.29	22.73	67.11	6.61	33.2	32.1	"	575.1	.0	322.0	.968	.00	7.30		4699.8
548	55.87	96.41	22.73	66.77	6.43	.0	38.5	"	246.5	.0	152.4	9.999	88.88	99.99		4785.1
548	55.22	96.53	22.77	66.42	6.25	.0	42.8	"	381.7	.0	141.7	9.999	88.88	99.99		4894.4
550	55.05	96.47	22.81	66.25	6.17	.0	51.4	"	328.6	.0	123.9	9.999	88.88	99.99		4961.7
552	55.05	96.34	22.87	66.22	6.18	.0	53.5	"	388.5	.0	93.0	9.999	88.88	99.99		4983.6
554	55.04	96.12	22.93	66.32	6.20	.0	44.9	"	349.2	.0	136.3	9.999	88.88	99.99		5003.0
556	55.26	95.93	22.96	66.54	6.31	.0	40.7	"	337.2	.0	132.4	9.999	88.88	99.99		4953.5
558	55.48	95.84	23.00	66.75	6.42	26.4	32.1	"	652.9	.0	197.7	1.210	.00	4.47		4902.7
600	55.69	95.76	23.04	66.93	6.54	12.9	25.7	"	487.8	.0	155.2	1.990	.00	5.83		4850.6
602	55.90	95.68	23.07	67.19	6.66	.0	21.4	"	275.6	.0	92.8	9.999	88.88	99.99		4800.5
604	56.10	95.60	23.11	67.43	6.77	.0	17.1	"	217.4	.0	103.5	9.999	88.88	99.99		4749.4
606	56.31	95.52	23.15	67.68	6.89	.0	15.0	"	172.9	.0	86.9	9.999	88.88	99.99		4697.2
608	56.37	95.30	23.20	67.69	6.94	22.8	12.8	"	251.6	.0	121.5	.563	.00	1.82		4683.1
610	56.29	94.94	23.27	67.67	6.93	309.3	17.1	"	19729.7	701.5	1054.4	.004	.16	.23		4705.3
612	56.02	95.04	23.31	67.39	6.77	1912.0	21.4	"	9072.7	212.3	1043.7	.011	.11	.50		4780.1
614	55.75	95.14	23.35	67.12	6.61	612.4	32.1	"	2824.5	64.6	504.9	.052	.11	.69		4855.4
616	55.47	95.25	23.38	66.88	6.47	194.3	38.5	"	1540.6	29.5	708.3	.209	.16	3.41		4931.9
618	55.20	95.37	23.42	66.55	6.32	145.7	51.4	"	1376.3	18.5	1198.2	.352	.13	7.60		5009.7
620	55.03	95.44	23.45	66.33	6.23	310.9	59.9	"	2447.9	33.2	837.6	.193	.11	2.44		5055.4
622	54.97	95.45	23.49	66.32	6.20	281.2	47.1	"	2242.4	33.2	1152.3	.167	.12	3.85		5067.7
624	54.91	95.47	23.53	66.26	6.17	307.7	42.8	"	1968.6	33.2	624.4	.139	.11	1.77		5078.8
626	54.98	95.43	23.56	66.34	6.21	376.6	47.1	"	2304.1	40.6	519.6	.125	.11	1.16		5047.6
628	55.19	95.34	23.60	66.55	6.32	445.6	51.4	"	2670.4	46.2	710.7	.115	.10	1.42		4974.7
630	55.40	95.25	23.64	66.77	6.43	439.2	53.5	"	2961.4	.0	817.1	.122	.00	1.68		4901.7
632	55.61	95.17	23.67	66.99	6.54	855.2	55.6	"	5101.2	.0	848.3	.365	.00	.90		4828.5
634	55.81	95.08	23.71	67.19	6.65	471.3	42.8	"	3047.9	.0	472.1	.061	.00	.84		4758.5
636	56.01	95.00	23.75	67.39	6.77	482.5	30.0	"	2841.6	57.2	437.1	.062	.12	.74		4688.4
638	56.21	94.92	23.78	67.59	6.88	317.4	21.4	"	2355.5	36.9	370.7	.067	.12	.92		4618.4
640	56.41	94.84	23.82	67.79	7.00	534.7	17.1	"	3569.6	64.6	432.6	.032	.12	.66		4548.4
642	56.62	94.74	23.86	68.00	7.13	77.7	15.0	"	342.4	.0	160.0	.193	.00	1.03		4476.5
644	56.82	94.64	23.90	68.21	7.26	70.5	12.8	"	297.8	.0	136.1	.182	.00	.80		4404.9
646	57.03	94.54	23.93	68.42	7.39	97.8	12.8	"	575.2	12.9	223.9	.131	.13	1.47		4333.5
648	57.23	94.44	23.97	68.63	7.53	158.7	10.7	"	1146.9	27.7	375.5	.067	.17	1.86		4262.5
650	57.44	94.34	.01	68.84	7.67	22.0	8.6	"	147.2	.0	139.5	.389	.00	2.70		4191.9
652	57.64	94.24	.04	69.04	7.82	117.8	6.4	"	380.9	.0	203.4	.055	.00	1.05		4121.8
654	57.85	94.14	.08	69.25	7.97	262.9	21.4	"	814.8	27.7	751.1	.081	.11	2.55		4052.1
656	57.92	94.55	.08	69.27	7.98	6068.7	21.4	"	24502.3	1513.9	1921.4	.004	.25	.30		4031.9
658	58.03	94.97	.07	69.29	8.00	176.3	10.7	"	992.9	18.5	704.7	.062	.11	3.62		4011.8
700	58.00	95.38	.07	69.31	8.01	689.3	42.8	"	3355.1	147.7	624.4	.062	.21	.79		3991.7
702	58.15	95.82	.06	69.32	8.02	197.9	38.5	"	13557.7	553.8	635.1	.195	2.80	2.81		3973.5

UT	GEOG. LAT.	GEOG. LONG.	MAG. TIME	INVAR. LAT.	L	WAVELENGTH 4278	4861	5200	5577	5995	6300	RATIO TO 4278 4861	5995	6300	REL INT	SHADOW HEIGHT
704	58.22	96.29	.05	69.32	8.02	280.5	42.8	"	1506.4	36.9	405.0	.153	.13	1.16		3957.0
706	58.29	96.75	.04	69.32	8.02	307.7	42.8	"	1506.4	36.9	405.0	.139	.12	1.06		3940.5
708	58.41	97.03	.05	69.39	8.07	3953.8	44.9	"	15047.0	738.5	1350.5	.011	.19	.32		3906.8
710	58.53	97.12	.07	69.54	8.18	90.4	47.1	"	671.0	332.3	1345.2	.521	3.67	13.49		3856.1
712	58.66	97.04	.10	69.63	8.25	.0	42.8	"	4587.7	166.2	917.0	9.999	99.99	99.99		3815.5
714	58.66	96.80	.16	69.67	8.28	708.6	36.4	"	3098.4	110.8	567.3	.051	.16	.69		3783.7
716	58.67	96.57	.22	69.71	8.32	789.6	32.1	"	3440.7	221.5	358.6	.041	.28	.35		3750.7
718	58.68	96.33	16.52	69.75	8.35			WINDOW CLOSED								3716.6
720	58.69	96.09	16.54	69.79	8.38			WINDOW CLOSED								3681.4
722	58.69	95.85	16.56	69.83	8.41			WINDOW CLOSED								3645.2
724	58.70	95.61	16.59	69.87	8.44			WINDOW CLOSED								3608.1
726	58.71	95.38	16.61	69.91	8.47			WINDOW CLOSED								3570.0
728	58.72	95.14	16.63	69.95	8.50			WINDOW CLOSED								3531.2
730	58.72	94.90	16.65	69.99	8.54			WINDOW CLOSED								3491.5
732	58.73	94.66	16.67	70.02	8.57			WINDOW CLOSED								3451.1
734	58.74	94.42	16.70	70.06	8.60			WINDOW CLOSED								3410.1

THE SPATIAL EXTENT OF AURORAE IN O(5577) AND N_2^+(4278) EMISSIONS

S. B. Mende
R. H. Eather

May 1970

This research was funded in part by NASA under Contract Number NASw 1997.

Lockheed Palo Alto Research Laboratory
3251 Hanover Street
Palo Alto, California 94304

ABSTRACT

An investigation of the spatial extent of aurorae was undertaken from College, Alaska, by the ground based Lockheed two channel (5577Å and 4278Å) image intensifier TV system and with a multichannel boresighted tilting filter photometer. The measurements indicate that even on clear nights the extinction due to scattering in the 4278Å is significant unless the measurements are taken at small zenith angles. To confirm the results and to avoid the low altitude scattering problem, measurements were made on a quite arc with the Lockheed 6 channel tilting filter zenith photometer during the NASA CV 990 expedition. These results show that in the cases observed there was no significant difference between the latitude profiles of O(5577) and N_2^+(4278) emissions.

INTRODUCTION

The most intense visible auroral radiations are produced by the OI(557Å) transition and by the N_2^+ band system. The spatial distribution of these two components of auroral emission has been investigated by Romick and Belon (1969, 1967a, 1967b) who obtained a very interesting result. In their experiment they measured the intensity profile of a thin auroral arc and concluded that the spatial width (the north south extent) of the emission is greater in the N_2^+ molecular ion emission than in the OI(5577) emission. This result was unexpected and a careful analysis was given by the authors who found that the discrepancy was real.

If the auroral arc investigated by Romick and Belon was typical, one should expect to find quite often a similar difference in the spatial width in auroral arcs. Since the investigation discussed in the present paper was an attempt to repeat this experiment it may be necessary to summarize the previous results to show whether or not a significant discrepancy was observed. According to Romick and Belon (1964, 1967a, 1967b) there are two distinct zones in which the N_2^+(3914) and the OI(5577) deviate in distribution. The auroral arc under investigation apparently consisted of an intense central core and of a diffuse broad "skirt" of less than 5% of the peak intensity. According to the model which fits the observations best both of these regions exhibited a difference in the spatial distribution of the two emissions. A characteristic halfwidth in the central core for the 3914 and 5577 was 5 km and 3.3 km respectively. This corresponds to an angular distance of 2.9° and 1.9° respectively as observed from the ground directly under the auroral form.

The low intensity skirt characteristic halfwidth was 31 km and 15 km in 3914 and in 5577 respectively (corresponding to 17^{o} and 8.5^{o}). Because of this structure and the differences in the distribution of the two intensities the ratio of the two emissions is a very complex function of position. Romick and Belon found that the ratio of volume emission rate varied between 1 and 12.

The Romick and Belon (1969, 1967a, 1967b) investigation was carried out by fitting photometer data from two stations to a model aurora. It was found that the adaptation of a model with the above described deviation in the 3914Å and 5577Å distribution was necessary to fit the experimental data. A critical review may show that there could be other models which would satisfy the observations. For example it is not evident why the luminosity distribution is necessarily symmetrical about the center of the arc in the north south direction. On the other hand it is not clear either that a non-symmetrical model would yield the desired results without the hypothetical 3914/5577 anomaly. Other criticisms could be raised against the treatment of scattering by Romick and Belon. For example one can show that the anomaly as observed in the broad "skirt" region of the arc could have been caused by atmospheric scattering.

Murcray, et al. (1967) conducted a rocket photometer experiment and apparently found similar discrepancy in the spatial extent of the N_2^+ and OI(5577) emissions. This rocket method did not produce a quantitative measure of the differences in the arc and the geometry of the experiment seems to hinder quantitative interpretation.

The excitation of the first negative band system of N_2^+ (3914Å or 4278Å) requires the presence of particles whose energies are in excess of 18 volts. Therefore the excitation of these emissions is caused mainly by primary particles. The cross sections are fairly well known for the ionization and excitation of N_2 allowing

the prediction of a fairly direct relationship between the energy distribution of the primary particles and the amount of light emitted in the N_2^+ negative band. The N_2^+ negative system therefore can be regarded as a faithful representation of the energy input of the primary auroral particles. Hence thetemporal and spatial distribution of the 3914Å or 4278Å emission in an auroral form can be regarded to represent the distribution of the primary energy input.

The generation of the 5577Å OI emission is a less well understood mechanism, Donahue, et al. 1968. The observation of the N_2^+ negative band system and its relationship to 5577Å emission may be able to resolve the mechanism responsible for 5577 generation.

The observed difference in the spatial extent by Romick and Belon (1967a, 1967b)(hence it will be referred to as "blue green anomaly") can be interpreted as a spatial variation in the 5577 generating mechanism across the auroral form. For example this could be caused by an inherent nonlinearity in the 5577 generation.

Alternatively the blue green anomaly could be caused by a spatial variation of either the incoming auroral primaries within the auroral form or the variation of the ambient atmosphere. If on the other hand the first hypothesis were true and an inherent non-linearity in the interaction itself were responsible for the anomaly one would expect to see the non-linearity in the 5577 green production quite generally in all intense auroral formations.

In an attempt to repeat the observation of the blue green anomaly two experiments were carried out. In the first experiment an image intensifier television system was used to record images of aurora simultaneously in 4278Å and in 5577Å emission. In the second experiment an airborne multichannel filter photometer was used to measure the 4278Å and 5577Å ratio while the photometer was scanning the edge of a steady "quiet arc" in the zenith.

DESCRIPTION OF THE IMAGE INTENSIFIER TV CAMERA

For optimum detection efficiency photoelectric detection techniques are used to investigate the aurora. In a photoelectric photometer the photons from the auroral luminosity are imaged on the photosensitive photocathode by an optical system. Thus the photocathode produces photoelectrons which can be counted and the count rates recorded. Table 1 summarizes quantitatively the maximum theoretical efficiency which is possible by using this technique. $P\alpha$ is the photoelectron count rate as a function of α the angular field of view. The substitution of practical parameters into the formulae gives the tabulated values of Table 1. Note that at the field of view which corresponds to the spatial resolution of a conventional TV system, i.e. less than 0.1 degrees, the photoelectron counting rate is 200 photoelectron counts per second for a 1 kilorayleigh aurora. Hence for a high time resolution TV system which takes 60 exposures per second the average number of counts in one field is only about 3. Such considerations show clearly that most real time fast auroral studies will necessitate the efficient recording of almost all of these photoelectrons. Even then the high time and spatial resolution restricts the investigation to the brighter events only and in most cases the results will be limited by statistical noise. There have been a number of investigations of auroras using modified conventional TV cameras such as Image Orthicons and SEC Vidicons. (Davis and Hicks 1964, Cresswell, et al 1965, Davis 1967, Mende and O'Brien 1968, Beach 1968, Mende 1969)

These investigations however were restricted to the recording of brighter events and using no spectral separation of the different wavelength emissions. In order to enhance the detection efficiency

as much as possible an Image Intensifier TV camera was constructed which has a very high photoelectron recording efficiency. (Mende 1970)

The system is illustrated on Fig 1. Light from the aurora is received through two channels. The direct channel passes through an interference filter of wavelength type 1. The other channel is reflected by the so called 40^{o} mirror and then the light passes through the interference filter of wavelength type 2. The two beams are then combined by the 45^{o} dichroic beam splitter. This 45^{o} mirror is coated with a reflector which is highly reflective to radiation type 2 while it is almost fully transparent to wavelength type 1. This way the two beams are recombined with minimum loss of light. Both beams are then passed through the primary optics and focused on the first photocathode of the Image Intensifier Tube. In order to re-separate the two beams the top half of the image intensifier photocathode is covered with a gelatine Wratten type colour filter which is transparent to type 1 light and opaque to type 2 light. While the bottom half is covered with a different Wratten filter which separates in the opposite sense.

By the adjustment of the angle of the 40^{o} mirror the two beams could be made to originate from the same part of the sky. This way the same aurora could be imaged through the two different filters to form the two channel color separation. For the experiments described in this paper the filter for beams 1 and 2 were selected to optimize the transmission of 5577 and 4278 respectively. The bandwidth of both filters was $60\mathring{A}$.

The photoelectron image in the image intensifier was focused by the aid of the focussing electro-magnet. The Image Intensifier could be made to operate with a light gain of over 10^{6} which was sufficient to generate a bright recordable light spot on the output phosphor for each photoelectron. However for most auroral intensity profile

analysis lesser image intensifier gains were found to be optimum. The image from the output phosphor was lens coupled into the Plumbicon type TV camera. The Plumbicon is very similar to vidicons however it is superior in linearity, time resolution and dark current. The camera generated video signal was recorded by magnetic recording with the time and angular position of the look angle. For more detailed description of a similar system see Scourfield and Parsons (1969).

The TV system was boresighted with a four channel tilting filter photometer of the type described by Eather and Reasoner 1968. The channels which were used to monitor 5577Å, 4278Å, 6300 OI and 4861Å.

Besides extensive cross calibrations of the two systems in the field the TV system was evaluated independently in laboratory tests regarding linearity, resolution and absolute sensitivity.

THE IMAGE INTENSIFIER TV CAMERA OBSERVATIONS

During March and the early part of April 1969 the Lockheed Image Intensifier Plumbicon Camera was used to gather auroral data at College, Alaska (invariant latitude of 64.9 and L = 5.5.) Many hours of video tapes were gathered during every clear night but no narrow auroral arc was ever observed near the zenith. The general pattern of the auroral activity fitted very well the quiet time auroral oval concept of Feldstein 1963 by displaying quiet arcs near the northern horizon during early evening and intensifying and becoming more active towards midnight while moving southwards. By the time the aurora was near the zenith it was generally fairly active approaching the break up phase. During the month and a half of observation periods there was not one single case of a quiet narrow arc near the zenith at College which was comparable in width to the one documented by Romick and Belon (1964, 1967a, 1967b).

Quite often auroral arcs were observed near the horizon during early evening periods. However the observation of the horizontal distribution of the N_2^+(4278Å) and OI(5577Å) in these arcs was hindered by the geometry and by the extremely high apparent extinction of the N_2^+(4278). It was found that even on clear nights the ratio of green to blue was very high (between 10 and 20) for aurora observed at zenith angles of greater than 60 degrees. (Normal 5577Å to 4278 ratios range between 4 and 6.) Such ratios can be explained on the basis of extinction due to aerosol scattering. Nevertheless since the transmission of the atmosphere was not monitored during these experiments any observations made at large zenith angles were considered suspect. In addition the very high extinction in the

blue 4278 made it very difficult to construct intensity profiles for the N_2^+ emission because of the very poor signal to noise ratio at normal auroral intensities.

The data analysis was restricted to events which occurred near the zenith and therefore contained a realistic blue to green ratio. Most of these events were however fairly active and were very unlike classical quiet arcs. Fortunately the high time resolution TV system was able to record these events and permit the interpretation of the instantaneous intensity profiles in the two emissions.

The visual observation of the TV monitor when the tape recordings of such events are replayed gives a very clear picture of the fast motions taking place in the 4278 N_2^+ emissions and clearly shows the slower changes in the 5577Å emissions which are presumably due to the lifetime of the parent state of the 5577 transition. A typical sequence from a zenithal auroral event is presented on Fig. 2. The photographs were taken at two second intervals and they are showing the time history of a small part of a fairly active broad zenithal auroral form. The field of view is essentially 15^o by 10^o for both colors. At the start of the sequence there is a broad auroral patch in the center which is decaying fast in the blue and slower in the green. Suddenly a very bright relatively narrow patch appears in the blue and moves towards the right of the picture. The green emission follows the blue profile with the characteristic time delay. In order to make a significant comparison of the time dependent profiles in the two colors a sequence of TV lines is presented in Fig. 3. The two TV lines correspond to the same point in space and represent the instantaneous profiles of the aurora in the two colors. The magnitude represents the intensity and was displayed with an attenuated amplitude in the green presentation. This was done to allow more direct comparison between the two profiles. The true ratio was near to six when corrections were applied for transmissions, etc.

The sequence shown on Fig. 3 shows very good agreement between the 4278Å and 5577Å profile. There is a distinct difference in the profile at 4 seconds after the beginning of the sequence, however the difference is in the opposite sense to the above mentioned "blue green anomaly." In our case the blue N_2^+(4278Å) is narrower than the diffuse OI(5577Å) emission distribution. This is expected from the long lifetime associated with the green emission. Prior to the exposure of this frame the 4278 distribution of the 4278Å emission was fairly broad. Later however it disappeared in the sides leaving the long lifetime green 5577Å emission persisting.

The follow-on part of the sequence consists of the blue patch moving towards the right and being followed by the green 5577 emission. This type of presentation permits the measurement of the apparent lifetime of the green 5577Å emission. However in order to interpret the real lifetime, height measurement and the estimation of quenching is required.

The above example shows that even in fast moving aurora the distribution of the N_2^+ 4278 and the OI 5577Å emissions are similar and the discrepancies can be resolved by arguments based on lifetime effects.

In the above experiment the signal to noise ratio was not high enough especially in the blue 4278 to resolve whether or not the extensive diffuse skirt (Romick and Belon 1967) was present. But regarding the question on the central core of the auroral form the very high spatial resolution of the TV system (less than .2 degrees) would have shown up a significant difference. It was a great advantage of the TV system that such studies could be carried out on fast moving aurorae and the arguments need not be restricted to quiet auroral forms. This is particularly important because auroral arcs which are seemingly quiet when examined by TV systems may show fine fast moving structures, Davis 1967.

Finally it should be pointed out that during the observations with the image intensifier TV camera several examples of rayed auroral arcs were recorded in which both the 5577 and the 4278 emissions showed rayed formations. The rayed or striated structure of the 4278Å is very good evidence to show that the primary auroral electrons are also structured in rayed forms. This shows therefore that the rayed structure of the visible aurora is generated outside the atmosphere which appears to contradict suggestions (Mende 1968) that auroral rays and striations in barium ion clouds may have similar origins.

AIRBORNE OBSERVATIONS

As it was pointed out earlier in this discussion, the scattering properties of the ever present aerosols in the lower atmosphere present a hazard in the observation of auroral intensity profiles. In order to make a definitive experiment aimed at the resolution of the "blue green anomaly" the photometric observation of the aurora from an aircraft was desirable. Such an opportunity presented itself during the 1969 NASA auroral aircraft expedition.

The Lockheed six channel photometer was flown on a Convair 990 jet aircraft. The photometer was mounted inside the aircraft and was looking through a plexiglass window which was mounted on the topside of the fuselage. The optic axis of the photometer channel was looking straight up in an approximately vertical direction when the plane was in flight.

The photometer was of the tilting filter variety described by Eather and Reasoner 1964 but for the purposes of this investigation the data was taken with fixed filters.

On the 7th of December 1969, the plane was flying in a near westerly direction and was flying parallel to a very well defined auroral arc in the zenith. The field of view of the photometer was generally north of the auroral arc except at times when the plane executed a slow roll motion in which case the photometer scanned the edge of the auroral arc.

Beside the Lockheed photometer there were a number of other instruments on the airplane, for example there were two TV systems which

were monitoring the aurora in the zenith in the entire visible. The video recordings taken by these cameras were used to illustrate the geometry of the aurora and the position of the field of view of the photometers.

On Fig. 4 a sequence from TV monitor photographs is presented. These were taken while replaying the NASA video tapes and superimposing the timing information. The circle representing the 3^{o} field of view of the photometer was superimposed on the photographs manually. This circle was found by measuring distances of stars on the TV monitor and computing the size of the area representing the 3^{o} circular field of view.

The important point to note is that during the sequence the field of view was never covered entirely by aurora and in fact the maximum overlap was never more than an area corresponding to less than 1.4^{o}. Therefore our photometric measurement in this case had a spatial resolution which was better than 1.4^{o}. This resolution compared very well with the resolution of the measurement of Romick and Belon (1964, 1967a, 1967b) who used effectively a 1^{o} field of view and were not observing directly overhead.

On Fig. 5 the photometer output is shown corresponding to the above event. The wide shape of the (6300Å) is due to diffusion effects associated with the very long lifetime of the O('D) state. The agreement between the traces representing the N_2^+(4278Å) and the OI(5577Å) emission is fairly evident.

To put the observation on a more quantitative basis, the variation of the ratio of 5577 and 4278 was studied. If there was a difference in the width of the arc in 4278 and in 5577 then the ratio of the two emissions would vary as a function of the distance perpendicular to the auroral arc.

Figure 6 represents a scatter plot of 5577Å intensity against 4278 intensity as the photometer was scanning the edge of the arc. The straight lines were hand fitted to establish the extreme ratios which could be yielded by such a scatter plot. The ratio did not vary significantly as the photometer scanned in and out of the auroral arc and this has to be interpreted that there was no difference between the extent of the auroral arc as observed in 4278Å and 5577Å.

In Fig. 7 another sequence is illustrated. In this case the maximum overlap of the photometer field of view approaches 2^{o}. The resultant photometer reading, Fig. 8, therefore shows a greater signal and therefore the corresponding scatter plot covers a larger intensity range (Fig. 9.) The ratio in this second case shows even less scatter. It is interesting to note that the two ratios derived from the scatter plots are not identical. Variation in the ratios of these two emissions are often observed. The reason for such variations could simply result from the changes in the primary auroral particle energy spectrum. Using this argument it may be perfectly possible that such energy spectrum may change near the edge of an auroral form and sometimes it could give rise to a change in the blue to green ratio. However if this were indeed the cause of the "blue green anomaly" then the occurrance of this phenomenon would probably be quite exceptional.

DISCUSSION

In two different experiments a search was undertaken for differences in the spatial extent of aurorae in N_2^+(4278Å) and OI(5577) emissions. Using a two channel narrowband filtered television system selected events were studied and beside fast temporal variations no systematic difference in the spatial profile of the two emissions was found. To confirm the findings an airborne photometer was used to obtain data concerning the profile of an auroral arc in the two emissions. These observations are apparently contradictory to earlier observations of Romick and Belon 1964, 1967a, 1967b, and Murcray 1967. Romick and Belon showed that a narrow auroral arc has a central core of 5577Å emission which is accompanied by a more diffuse body of N_2^+. In addition to this they found a broad region or "skirt" extending north south of the auroral arc which also consisted of a diffuse region of N_2^+ emission with a more centralized 5577 region. The intensity distribution in this latter diffuse broad region may well be explained by aerosol scattering because the blue N_2^+(3914) would be scattered preferentially. However regarding the difference in the more intense central region no explanation could be offered at present. The aurora under observation in each case may have been indeed different. The significance of the present work is in pointing out that the model proposed by Romick and Belon 1967a, 1967b may not be as commonly occurring a phenomenon as it was thought previously.

ACKNOWLEDGEMENTS

The authors are especially grateful to Dr. J. E. Evans for his continued interest and support throughout the progress of this work. We would like to thank the University of Alaska for providing the observatory facilities. Special thanks are due to Drs. T. N. Davis and G. J. Romick for their help and valuable comments in our numerous discussions. We gratefully acknowledge the cooperation of J. McGuire of NASA, Huntsville, for providing the airplane expedition video data. Thanks are also due to Louis Haughney of the NASA Airborne Science Office for his special efforts in assisting the experimenters during the NASA airborne expedition.

This research was supported in part by NASA under contract number NASw 1997 and by the Lockheed Independent Research Program.

REFERENCES

R. Beach, G. R. Cresswell, T. N. Davis, T. J. Hallinan and L. R. Sweet, "Flickering, a 10-cps fluctuation within bright auroras," Planet. Space Sci. 16, 1525-1529, 1968.

G. R. Cresswell, C. S. Deehr, and T. J. Halliman, "Television system for auroral research," University of Alaska, Sci. Rept. UAG R-172, NASA Contract NAs-5-9065, 1965.

G. R. Cresswell and T. N. Davis, "Observation on pulsating auroras," J. Geophys. Research, Vol. 71, p. 3155, 1966.

T. N. Davis and G. T. Hicks, "Television cinematography of auroras and preliminary measurement of auroral velocities," J. Geophys. Research, Vol. 69, pp. 1931-1932, 1964.

T. N. Davis, "Cinematographic observation of fast auroral variations," in Aurora and Airglow, B. M. McCormac, Ed. New York: Reinhold, pp. 133-141, 1967.

T. M. Donahue, T. Parkinson, E. C. Zipf, J. P. Doering, W. G. Fastie and R. E. Miller, "Excitation of the auroral green line by dissociative recombination of the oxygen molecular ion: analysis of two rocket experiments." Planet. Space Sci. 16, pp. 737-747, 1968.

R. H. Eather, D. L. Reasoner, "Spectrophotometry of faint light sources with a tilting-filter photometer," Appl. Optics, 8, pp. 227-242, 1969.

Y. I. Feldstein, "Some problems concerning the morphology of auroras and magnetic disturbances at high latitudes," Geomagnetism and Aeronomy, 3, p. 183, 1963.

S. B. Mende and B. J. O'Brien, "A high sensitivity satellite borne television camera for the detection of auroras," Appl. Opt. Vol. 7, pp. 1625-1634, 1968.

S. B. Mende, "A low light level slow scan TV camera for satellite application." Proc. IEEE, 57, 281-291, 1969.

S. B. Mende, "Single photoelectron recording by an image intensifier TV camera system," Proceedings of Symposium entitled: Astronomical Use of Television Type Image Sensors. To be published.

W. B. Murcray, "Spatial relationship of auroral OI and N_2^+ emissions," J. Geophys. Res., 72, pp. 1047-1051, 1967.

G. J. Romick and A. E. Belon, "The determination of the spatial distribution auroral luminosity," University of Alaska, Final Report, NSF G15725, NSF, Washington, D.C., May 1964.

G. J. Romick and A. E. Belon, "The spatial variation of auroral luminosity I. The behaviour of synthetic model auroras," Planet. Space Sci. 15, pp. 475-493, 1967a.

G. J. Romick and A. E. Belon, "The spatial variation of auroral luminosity II. Determination of volume emission rate profiles," Planet. Space Sci. 15, pp. 1695-1716, 1967b.

M. W. J. Scourfield and N. R. Parsons, "An image intensifier-vidicon system for auroral cinematography," Space Sci. 17, pp. 75-81, 1969.

Table 1

Number of photoelectron counts $P\alpha$ as a function of α the angular field of view.

$$P\alpha = \frac{10^9 \, T \, D^2 \, \alpha^2 \, \epsilon}{16} \text{ photoelectron sec}^{-1} \text{ kiloRayleigh}^{-1}$$

where

D = diameter of circular collecting optics (5 cm)

T = transmission of optics and filters (50%)

ϵ = photocathode efficiency (10%)

α = field of view (square) in radians

(For TV α = angular size of resolution element)

	$\alpha = 3^o$	$\alpha = 1^o$	$\alpha = .1^o$	α = 0 083 (Lockheed TV)
1 KR	$2 \cdot 4 \times 10^5$	$2 \cdot 7 \times 10^4$	$2 \cdot 7 \times 10^2$	2×10^2 (3 per TV field)
10 KR	$2 \cdot 4 \times 10^6$	$2 \cdot 7 \times 10^5$	$2 \cdot 7 \times 10^3$	2×10^3 (30 per field)
100 KR	$2 \cdot 4 \times 10^7$	$2 \cdot 7 \times 10^6$	$2 \cdot 7 \times 10^4$	2×10^4 (300 per field)

Each TV field is $\frac{1}{60}$ sec duration.

FIGURE CAPTIONS.

1. The Lockheed Image Intensifier Plumbicon Camera System.

2. Selected auroral sequence.

3. Video signal from each channel representing intensity distribution of TV lines shown on Fig.2.

4. NASA TV data from flight no.9 with photometer field of view superimposed.

5. Lockheed photometer data from flight no.9.

6. Scatter plot of 4278Å and 5577Å intensities.

7. NASA TV data from flight no.9 with photometer field of view superimposed.

8. Photometer data from flight no. 9.

9. Scatter plot of 4278Å and 5577Å intensities.

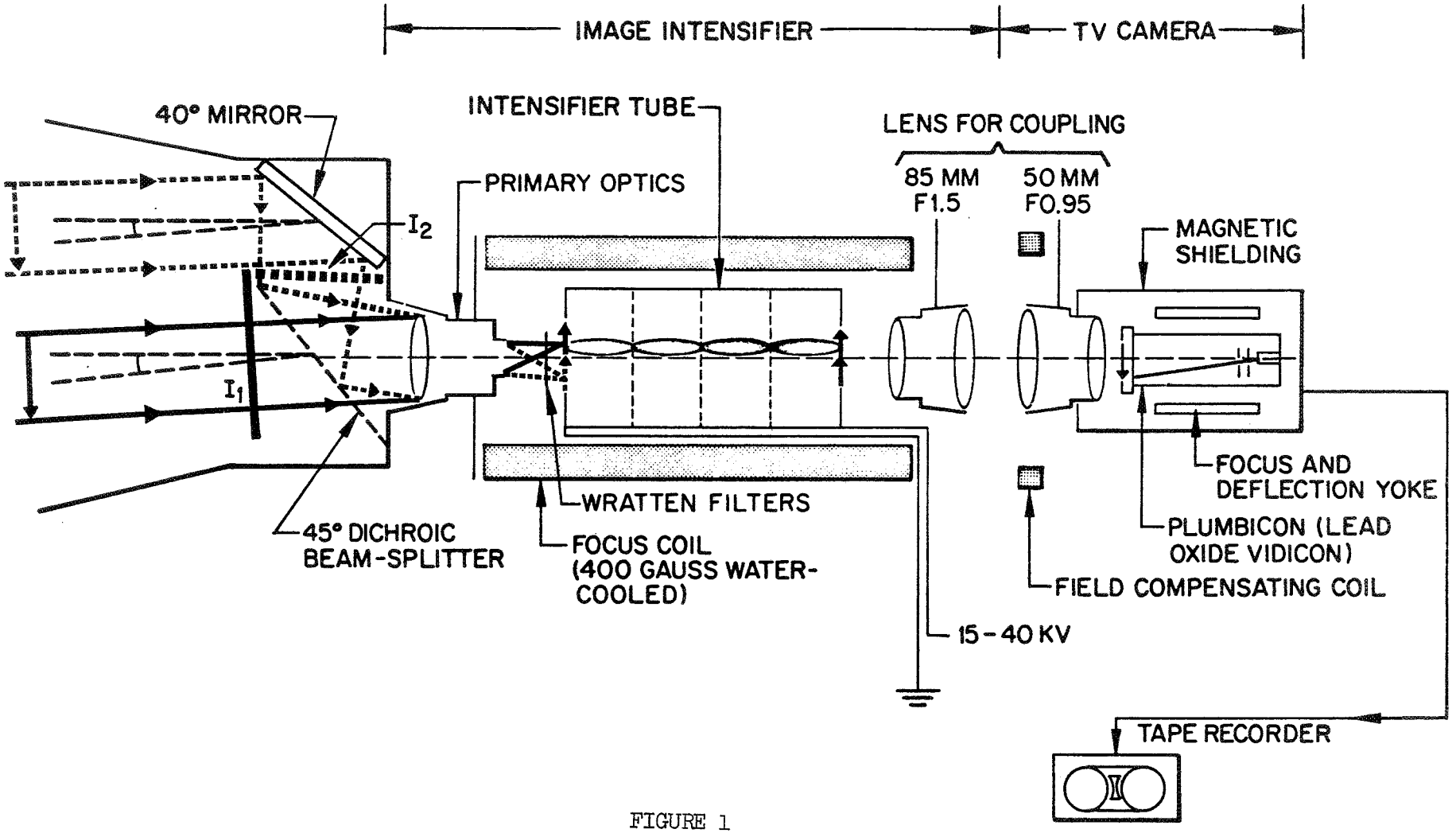

FIGURE 1

The Lockheed Image Intensifier Plumbicon Camera System.

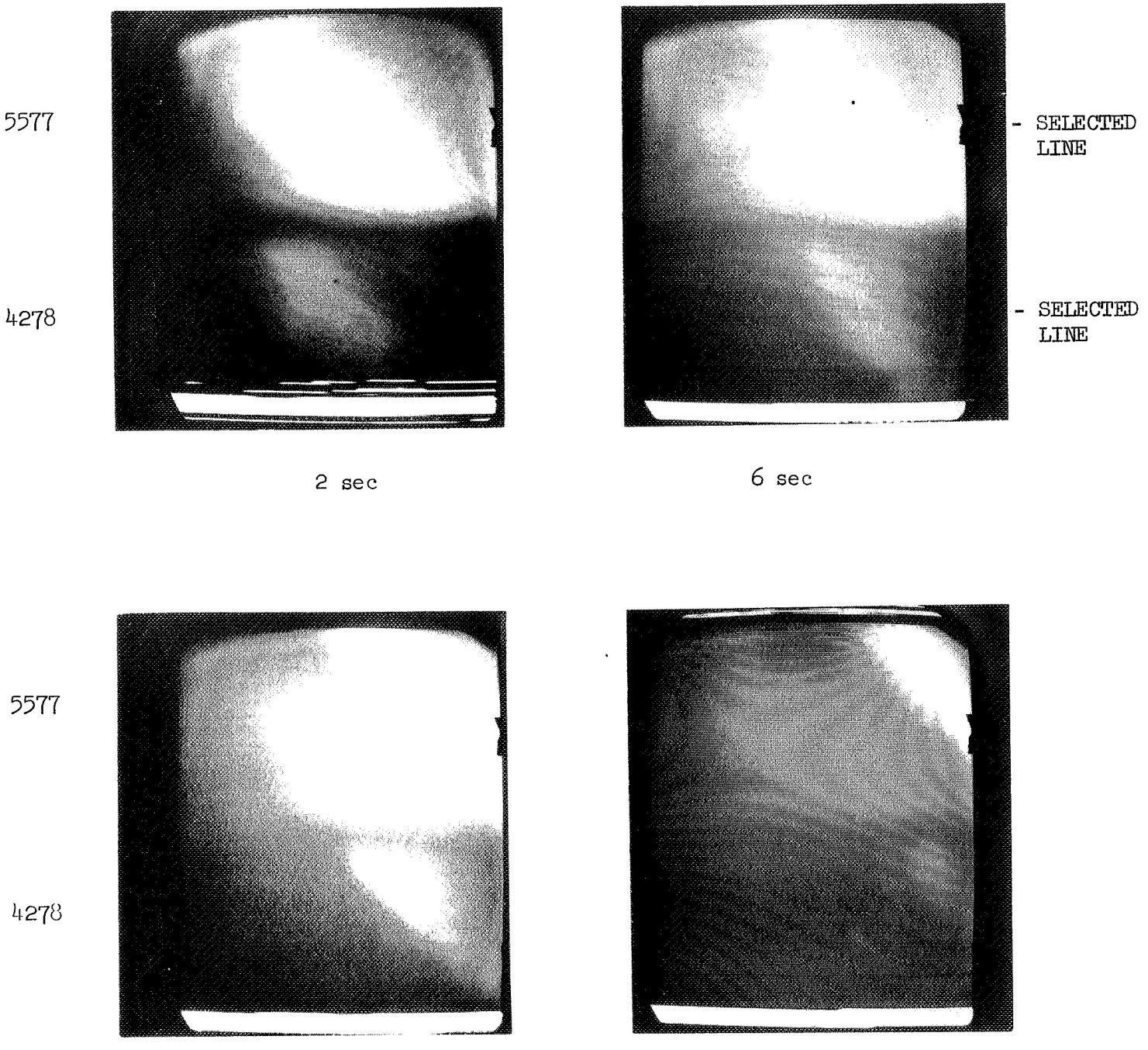

FIGURE 2. Selected Auroral Sequence.

TIME SEQUENCE

N_2^+ (4278) DISPLAYED AT 0.5 V/cm

OI (5577) DISPLAYED AT 2 V/cm

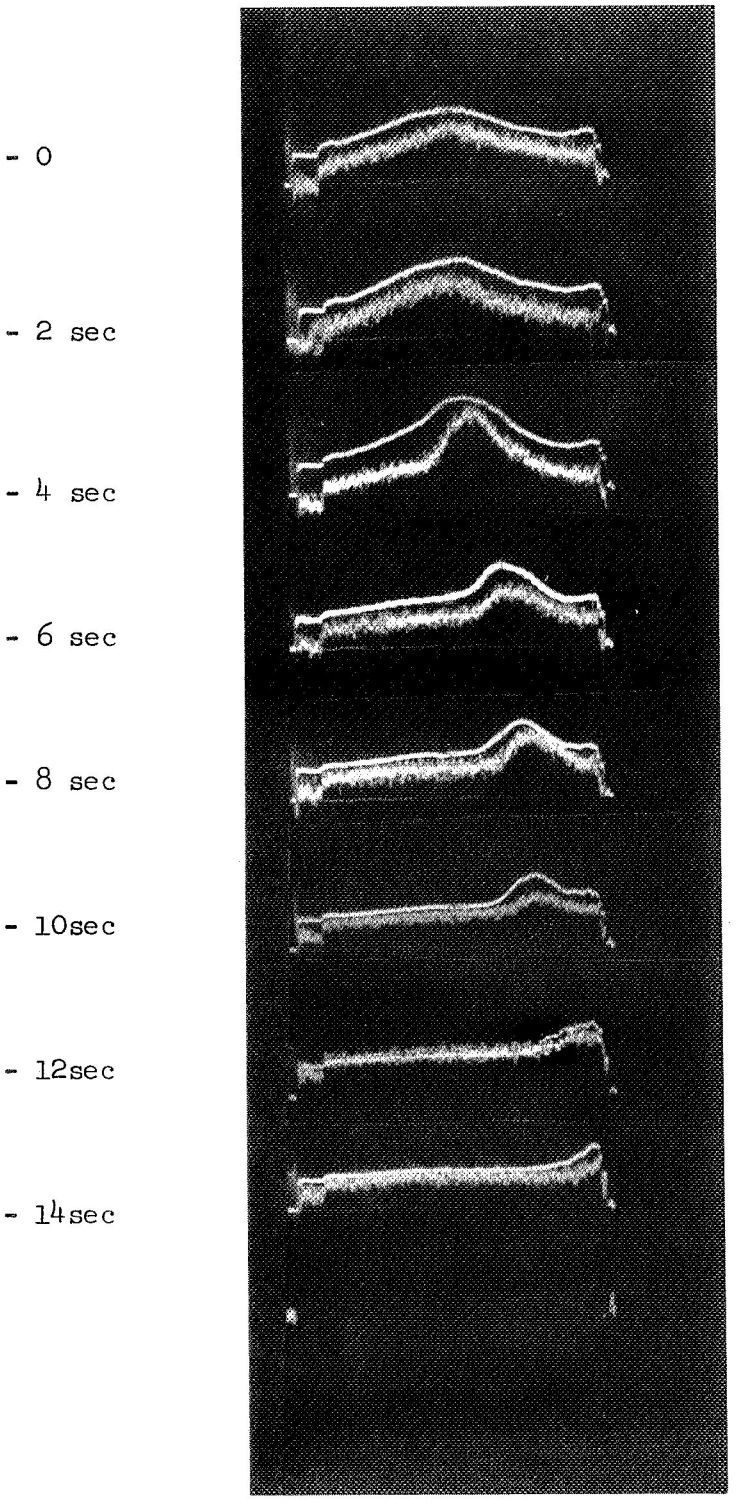

FIGURE 3

Video signal from each channel representing intensity distribution of TV lines shown on Fig. 2.

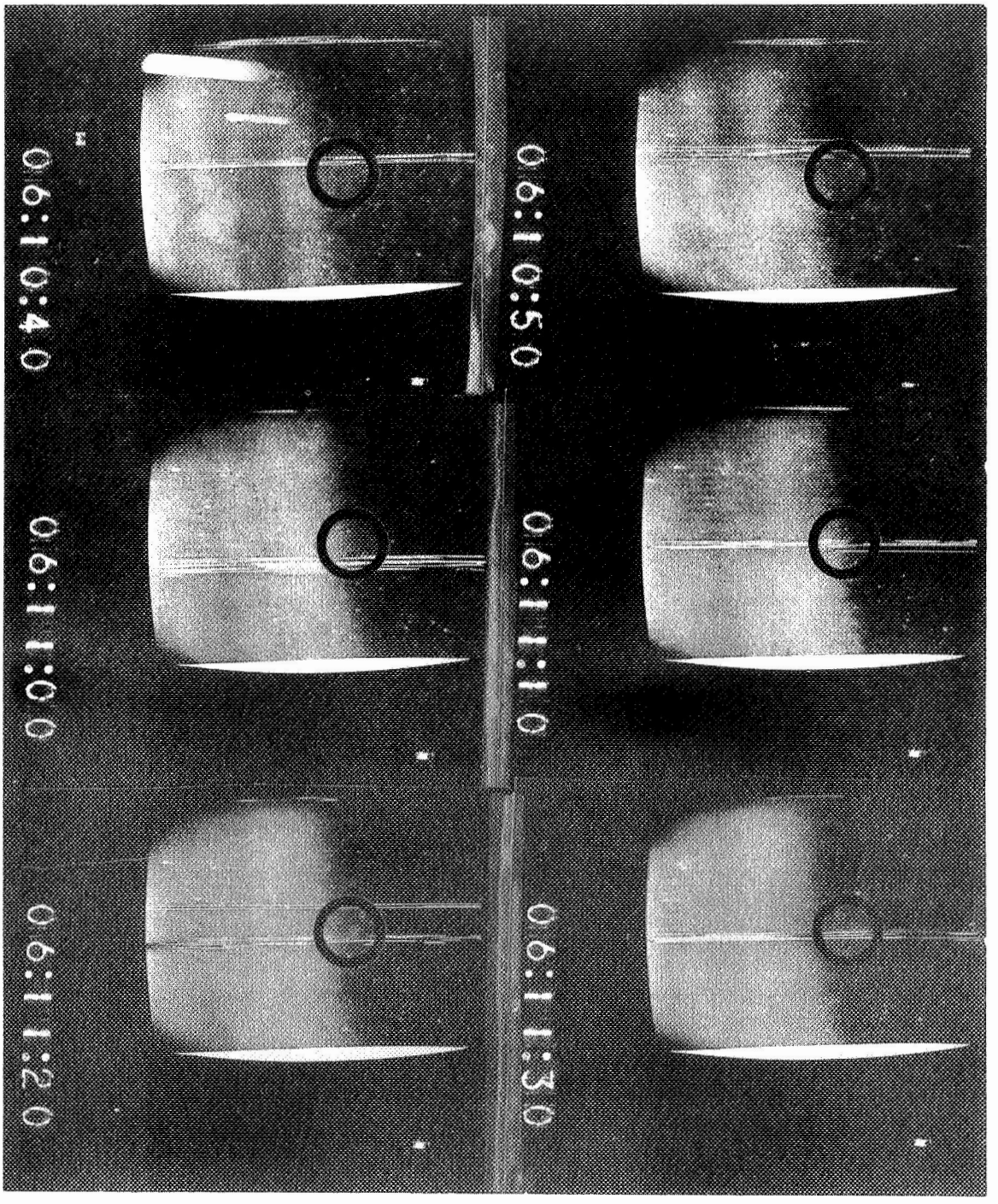

FIGURE 4

NASA TV data from flight no. 9 with photometer field of view superimposed.

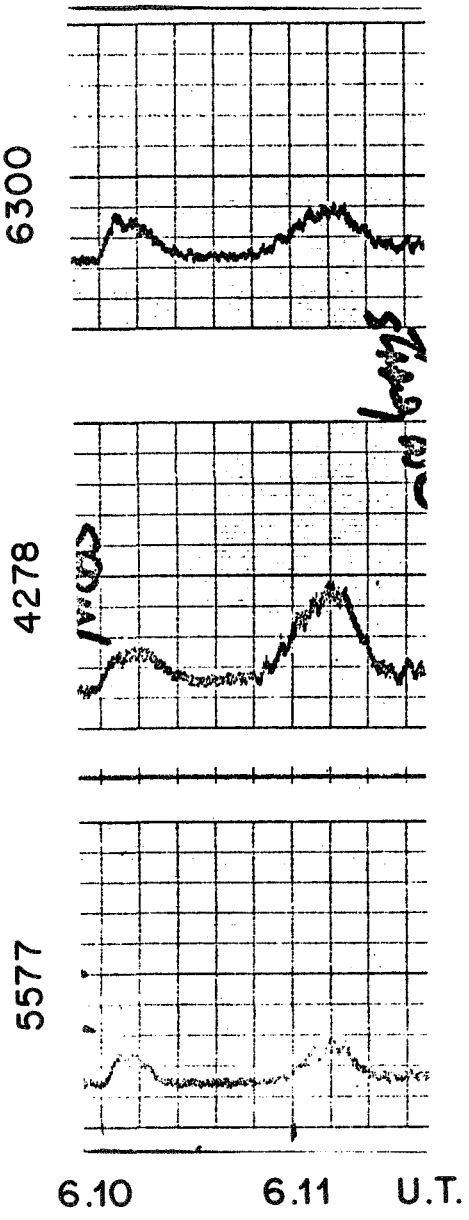

FIGURE 5

Lockheed photometer data from flight no. 9.

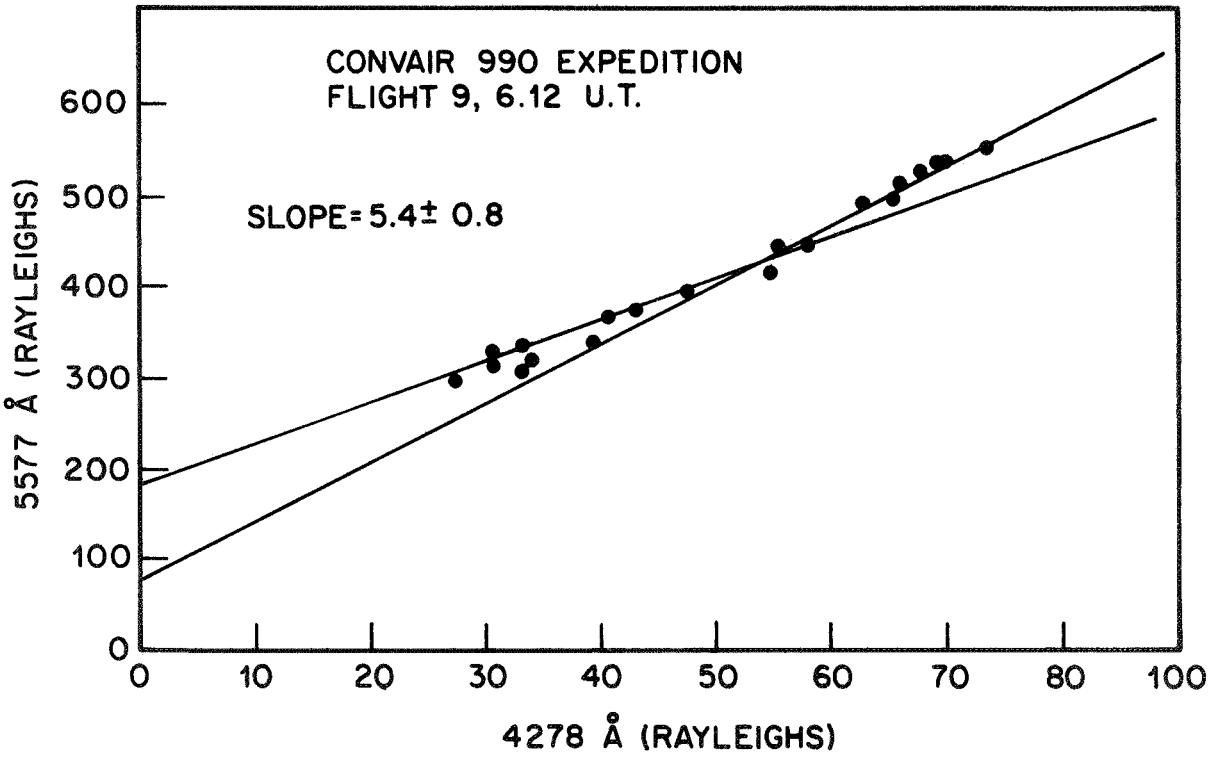

FIGURE 6

Scatter plot of 4278Å and 5577Å intensities.

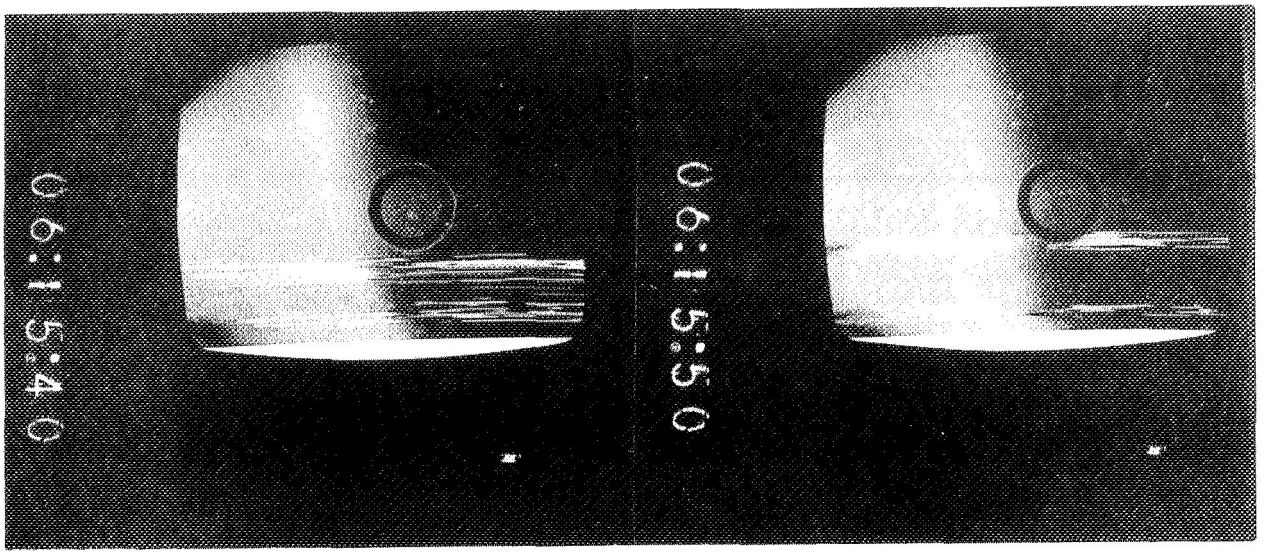

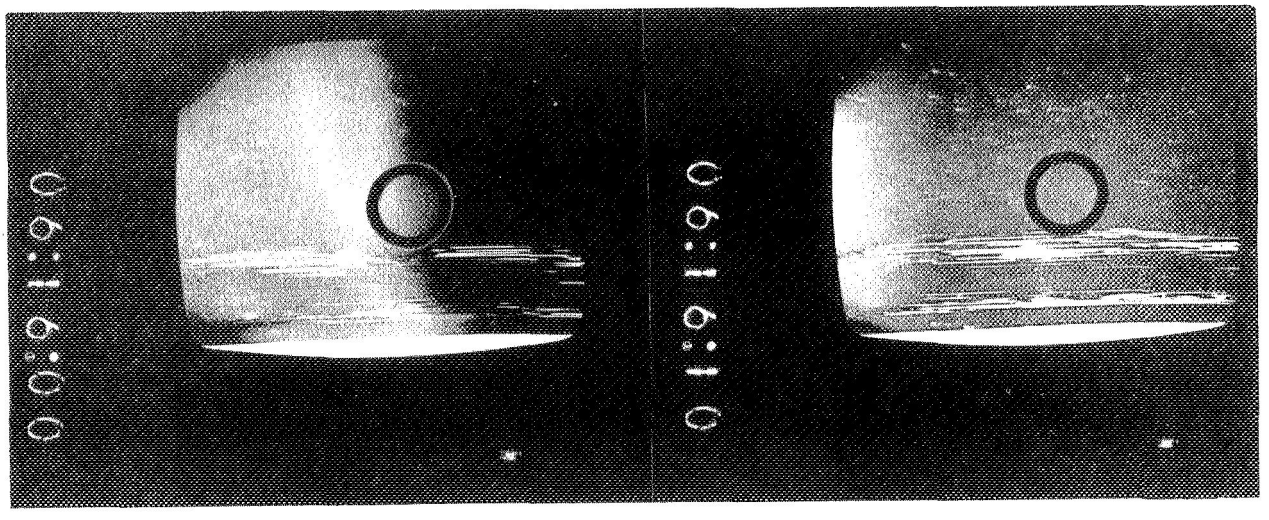

FIGURE 7

NASA TV data from flight no. 9 with photometer field of view superimposed.

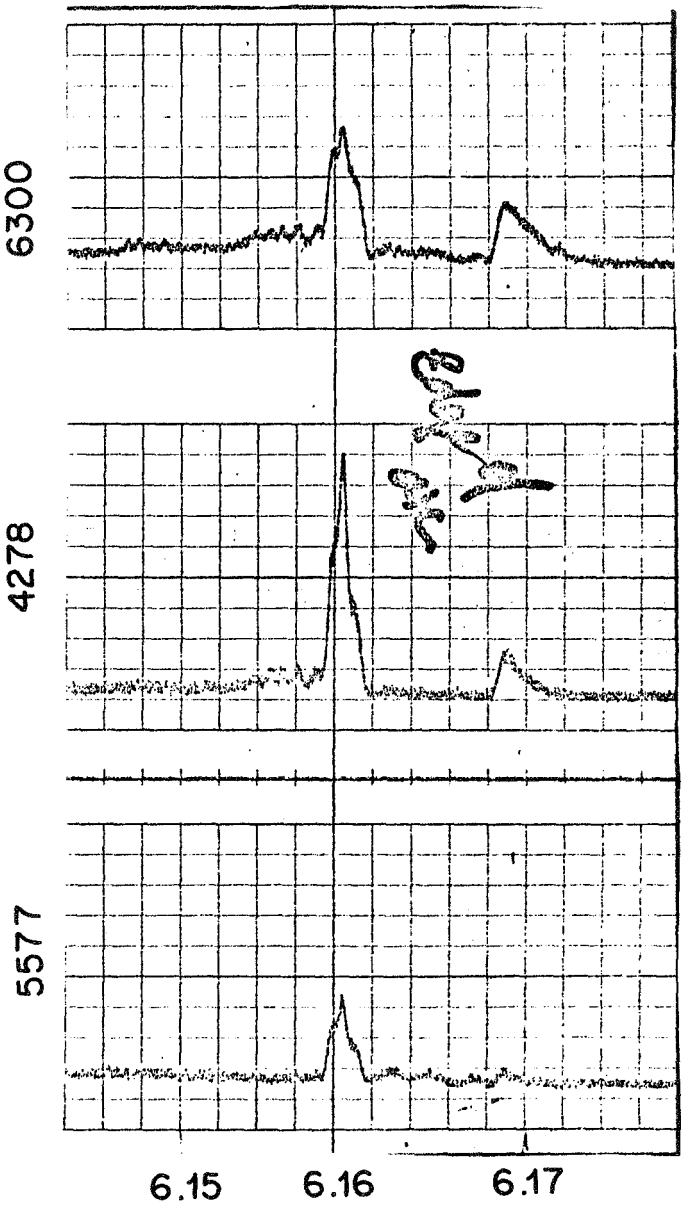

FIGURE 8

Photometer data from flight no. 9.

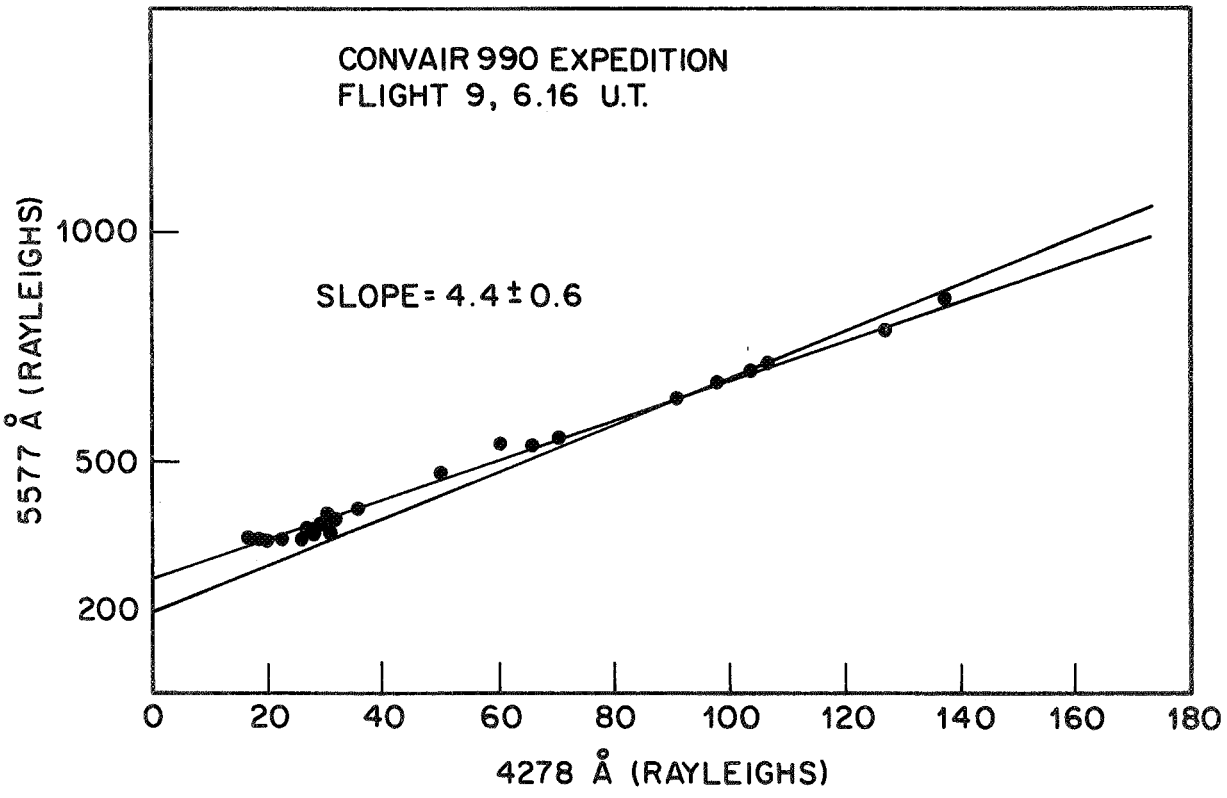

FIGURE 9

Scatter plot of 4278Å and 5577Å intensities.